SFWMD

SOUTH FLORIDA WATER MANAGEMENT DISTRICT

TECHNICAL PUBLICATION 88-7

June 1988

CALOOSAHATCHEE ESTUARY HYDRODYNAMICS

SOUTH FLORIDA WATER MANAGEMENT DISTRICT
SOUTH FLORIDA WATER MANAGEMENT DISTRICT
SOUTH FLORIDA WATER MANAGEMENT DISTRICT
SOUTH FLORIDA WATER MANAGEMENT DISTRICT
SOUTH FLORIDA WATER MANAGEMENT DISTRICT

TECHNICAL PUBLICATION 88-7

CALOOSAHATCHEE ESTUARY HYDRODYNAMICS

by

Panagiotis D. Scarlatos

June 1988

Water Resources Division
Resource Planning Department
South Florida Water Management District

EXECUTIVE SUMMARY

The Caloosahatchee estuary is an important environmental and hydrologic system in south-west Florida. The system is connected to Lake Okeechobee through the Caloosahatchee River canal and thus it is affected by regional water management policies. Human activities like urbanization, boating, fresh water discharges, and agricultural runoff can disturb the ecological balance of the system and cause its deterioration. The magnitude of the impact that a particular activity might have on the estuary cannot be easily assessed. To study the response of the estuary to a particular human-induced cause, other physical mechanisms which control the dynamics of the estuary must be properly documented and understood. Those physical mechanisms include tides, winds, direct precipitation, evapo-transpiration, ground water seepage, and surface runoff. The relations between these mechanisms and their impact on the ecosystem is time-dependent and very complicated; however, certain simplified assumptions can be introduced so that the system can be adequately studied for all practical purposes. For that purpose, field data must be collected and analyzed, and a model, either numerical or physical, must be developed so that the various physical processes can be simulated.

In the present study, the only water management activity that has been considered is the release of fresh water from Franklin Dam and its effect on the salinity distribution of the estuary. Excessive fresh water discharge can reduce the salinity levels substantially, while zero discharges during the dry season of the year might cause hypersaline conditions. Both hyper- and oligosaline conditions are undesirable since they can put stress on the estuarine flora and fauna. Due to the particular geometrical features of the estuary (shallow and elongated) two simplifying assumptions can be introduced for modeling purposes: the water motion is restricted along the main axis direction of the estuary, and the water velocity is uniform along the depth. Qualitative analysis of field data indicated that the most important physical driving forces are the tides, winds, and fresh water releases.

Lack of data prevented any detailed study of the impact of the other physical mechanisms, although their effect is expected to be of minor importance. Based on these assumptions a finite difference numerical model has been developed which simulates the water surface elevation, water velocities, and longitudinal salinity distribution under different hydrologic conditions. By changing the input parameters, various anticipated physical scenarios can be simulated. Thus, the most desirable situation can be assessed and a management program can be developed. The model operates on an IBM-PC compatible computer and it is written in BASIC language.

This project is the first phase of a two-phase study. The first phase includes the development of the mathematical Caloosahatchee River estuary dynamic model The second phase will be conducted in cooperation with the Environmental Sciences Division – after collection of environmental and biological data has been completed – and it will provide a management plan with a schedule for regulatory fresh water releases from the Franklin Dam.

TABLE OF CONTENTS

LIST OF FIGURES

LIST OF TABLES

ABSTRACT

The Caloosahatchee estuary dynamics have been simulated by means of a numerical model. The mass continuity and momentum balance equations have been applied to describe the water motion, and the advection-dispersion equation was used to model the longitudinal salinity distribution. The effects of astronomical tides, wind stresses, fresh water releases, and surface runoff were incorporated. The model will be used for the development of a management plan regarding the effects of fresh water discharges from Structure 79 on the salinity levels and consequently to the estuarine ecosystem.

KEY WORDS
Ecosystem; estuary; fresh water discharge; mathematical modeling; salinity; tides; winds.

INTRODUCTION

One of the most important areas within a coastal zone is the estuary. An estuary is a semi-enclosed body of water, freely connected with the open sea, where substantial mixing of salt and fresh water is taking place (Prichard, 1967). Serving as a link between land and sea and being ideal for fishing, transportation, and recreation, estuaries have always been heavily populated. Unfortunately, intensive human interference with estuarine water has, in many cases, caused environmental and ecological problems. The limited flushing capacity of estuaries, the wide diversity of biological species, and the variety of human activities creates a very complicated system. Effective and efficient management of this system is not an easy or explicit task.

Each estuary is a unique, dynamic system subjected to a variety of controlling elements such as tides, winds, direct precipitation, surface runoff, and base flow. Substantial changes in any of these elements may cause imbalance of the existing estuarine conditions. Identification and quantification of the effects of each controlling element is very important but also very difficult. The combined effect is nonlinear and time dependent, and often many aspects are not well understood. The system is further complicated by human interference such as dredging, filling, and fresh water diversions.

Study of any estuarine system requires an extensive synoptic data base. These data should include information regarding hydrodynamics, meteorology, climatology, geomorphology, geology, human activities, and physical, chemical, and biological characteristics of the estuarine water. Temporal and spatial variability of the system will dictate the time and place that the data must be recorded. Analysis of the data will indicate the short and long period fluctuations of the estuarine features, reveal its physical trends, and establish cause-response relationships.

Simulation of estuarine systems is feasible by means of mathematical, physical, or analog model techniques (Mahmood and Yevjevich, 1975). With the advancement of digital computer technology, the main emphasis is placed on mathematical modeling. Physical models are very expensive and impose scale distortion problems, while analog simulation has very limited applicability. In mathematical modeling the system is idealized so that it can be represented by a set of equations. After proper boundary and initial conditions are assigned, solution is sought by means of a numerical algorithm.

Before developing any mathematical model, a qualitative analysis of the existing data should be conducted and the most important aspects of the system must be identified and addressed (Scarlatos and Morris, 1986). Since the hydrodynamics of an estuary control the physical processes that occur within the system, the first step is to define water levels and current velocities. Once the hydrodynamics have been established, any other process can be simulated based on the hydrodynamic information. Understanding the physical behavior of the system is very important, because many unnecessary complications can be simplified by using proper assumptions. Also, consistency between the degree of accuracy of the governing equations and controlling physical quantities must be maintained so that no under-estimation or over-estimation of a certain physical process occurs within the overall phenomenon.

Purpose of This Study

The purpose of this study is to present a numerical mathematical model for the description of the Caloosahatchee estuary dynamics. The model is based on the concepts of mass and momentum balance for the hydrodynamics, and on the mass conservation principle for the salinity distribution. The model is one-dimensional and incorporates the effects of tides, winds, and fresh water discharges. The area under study is the section of the river extended between Shell Point at the river mouth and Franklin Dam (Structure 79). Due to shallow depths and the elongated form of the estuary, the equations utilized are those used for simulation of long period waves, i.e., the ratio between water depth and wave length is very small.

A large volume of data exists pertaining to the hydrology and hydrodynamics of the Caloosahatchee estuary. These data vary in location and are scattered through extended periods of time. Thus, before their utilization, the data were analyzed and interpreted for modeling purposes. The data were used for defining the boundary conditions of the system, for providing information for parameter calibration, and for verifying the model. Since there was no evidence supporting any substantial movement of the bottom material of the Caloosahatchee River, the study is limited to rigid-bottom hydrodynamics simulation.

When the effects of certain components of the system can not be directly assessed due to either lack of data or complexity of the nature of the component, then a sensitivity analysis is conducted to establish the range of influence that this component is expected to have on the system. Such sensitivity analyses can

be accomplished by varying the input parameters of the mathematical model or even comparing the physical system with other known systems of similar characteristics.

During the study, special effort has been placed on developing a comprehensive but also simplistic model with user-friendly computer codes which can run on a personal computer (PC). The programming language is BASIC. Both S.I. and U.S. Customary systems of units are utilized throughout this study.

PHYSICAL CHARACTERISTICS OF THE CALOOSAHATCHEE ESTUARY

Geographical Features

The Caloosahatchee River is located in Lee, Hendry, and Glades Counties of southwest Florida, extending from Lake Okeechobee to the Gulf of Mexico. The eastern portion of the river between the towns of Olga and Moore Haven is a canal (C-43) regulated by three structures. These structures are the Franklin Lock and Dam (S-79), the Ortona Lock (S-78) and the Moore Haven Lock (S-77), (Figure 1). This study includes only the portion of the river located west of S-79. This part of the river is freely connected with Gulf of Mexico tidal waters and has the features of an estuary. The boundary conditions at the eastern end of the estuary coincide with the regulated water releases from the Franklin Dam. The western boundary of the estuary is specified by the cross section between Shell Point and Cattle Dock Point near San Carlos Bay (Figure 2).

The majority of the estuarine banks are residential, and there are two major urbanized areas, the cities of Fort Myers and Cape Coral. The estuary is crossed by five bridges, at Cape Coral (fixed bridge), Fort Myers Edison (bascule bridge), Fort Myers US 41 (fixed bridge), Beautiful Island (bascule bridge), and Orange River (fixed bridge). The most important tributary is the Orange River, but there is an extensive network of channels directly connected with the estuary in the area of the city of Cape Coral which affects the dynamics of the system, acting like a storage area. A dredged navigation channel is maintained along the estuary. The part of the estuary east of Beautiful Island is much narrower and substantially deeper than the rest of the estuary.

A detailed representation of the Caloosahatchee estuary with all the pertinent geographic information is given in Figure 2.

Climatological Information

The climate of the Caloosahatchee estuary area is classified as subtropical. The annual average temperature is about 23° C (73° F) with monthly averages ranging from near 17° C (63° F) in winter to near 28° C (83° F) during summer. Winters are mild with warm days and moderately cool nights. Occasional cold fronts can bring temperatures near 0° C (32° F), but very seldom to freezing levels. During summer average maximum temperatures are mostly around 32° C (90° F) and, under rare circumstances, maxima have reached 38° C (100° F).

Rainfall averages over 125 cm (50 inches) annually, with heaviest precipitation during the summer. Based on precipitation, a 'wet' and a 'dry' period can be established. During the 'wet' period, which extends from June to October, the average monthly precipitation is over 20 cm (8 inches). In the 'dry' season, i.e., November through May, the average monthly precipitation is less than 5 cm (2 inches) for November to January and little more than 5 cm (2 inches) from February to May. There are frequently long periods during winter with little or no rainfall. In summer most of the rains occur in late afternoon or early evening hours and are of short duration but high intensity. In case of tropical storms or hurricanes passing close to the area, rainfall can reach 15 to 25 cm (6 to 10 inches) in one day. Thunderstorms are infrequent from November to April but they occur on an average of two out of three days from June through September.

The prevailing winds are from the east with moderate velocities of 11.2 km/h (7 mph) to 14.4 km/h (9 mph). Winds of 160 km/h (100 mph) associated with the passage of a hurricane have been recorded. In fall months the probability of a hurricane occuring is approximately 8 percent.

The relative humidity is very high within the area. During the day it ranges from 50 to 60 percent, while during the night it rises to an average of 80 to 90 percent.

The mean values of temperature, precipitation, winds, and relative humidity for Ft. Myers are given in Table 1.

Geometric Characteristics

The Caloosahatchee estuary is elongated in shape, extending approximately for 42 kilometers (26.25 miles) from San Carlos Bay northeast to Franklin Dam. The width of the estuary is irregular,

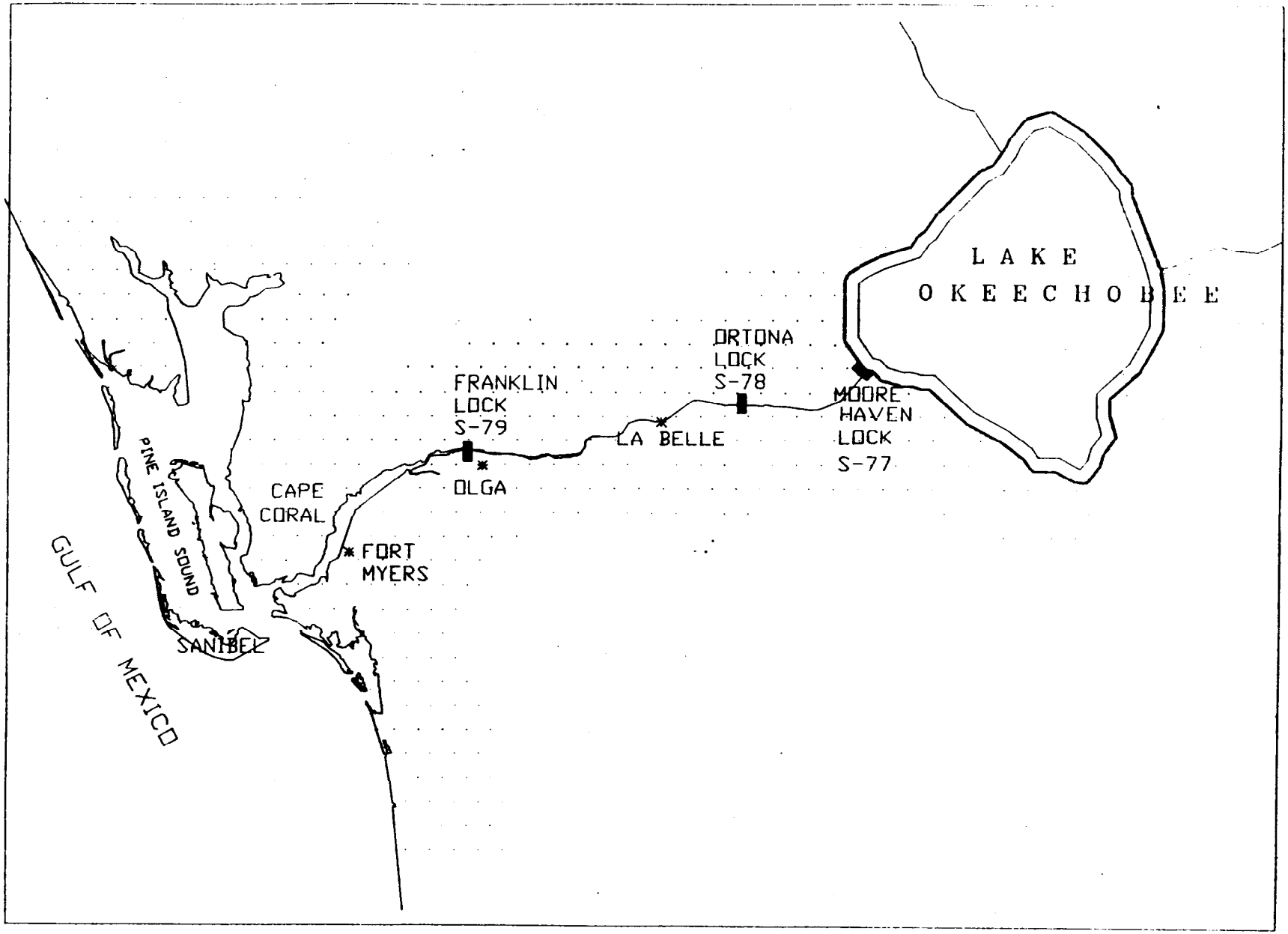

FIGURE 1 General Plan View of the Caloosahatchee River

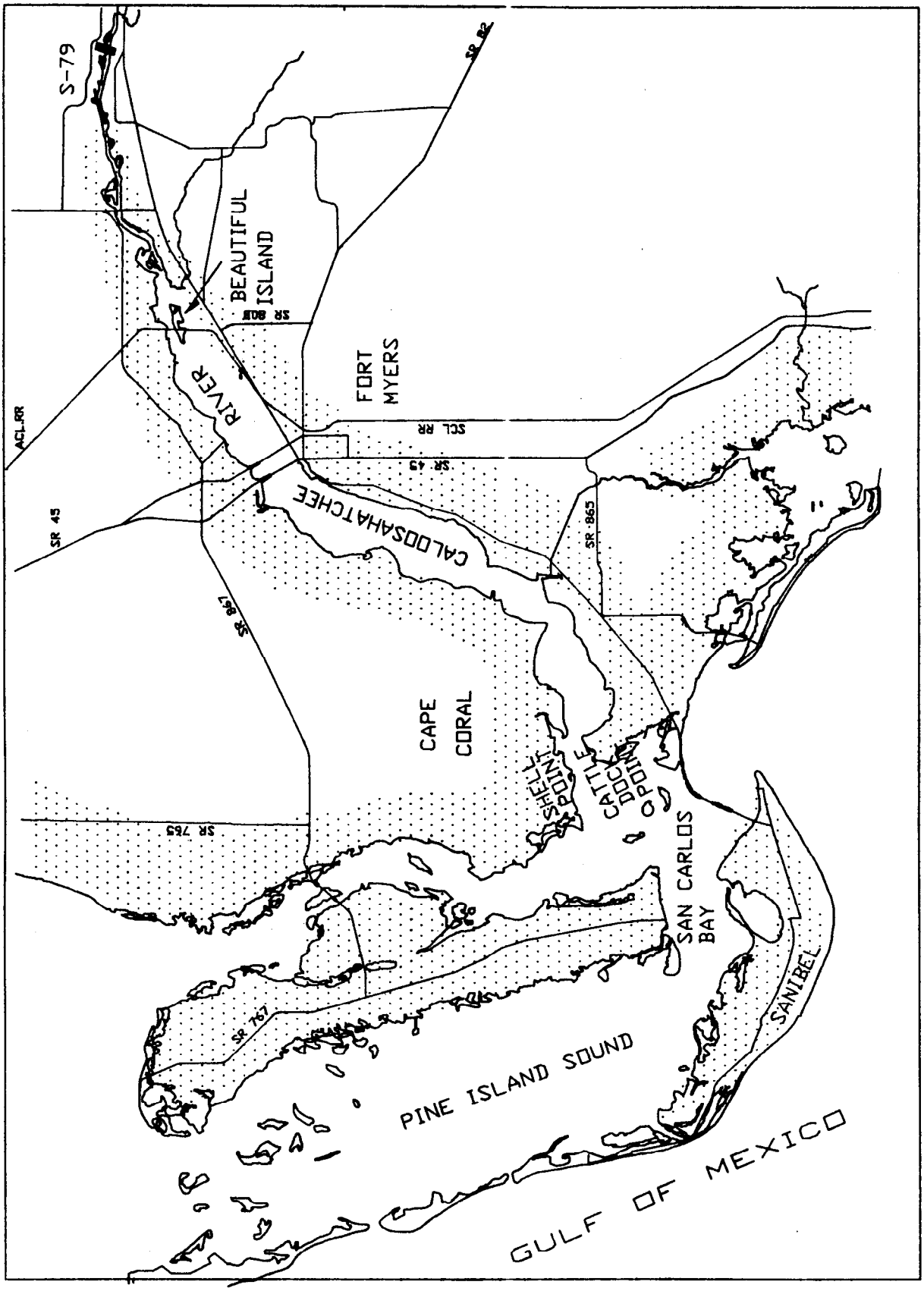

FIGURE 2 Detailed Plan View of the Caloosahatchee River

TABLE 1. Normal Monthly Values of Temperature, Precipitation, Winds, and Relative Humidity at Ft. Myers

Month	Temperature		Precipitation		Winds			Relative Humidity Local Hour			
	°C	°F	cm	In.	km/h	mph	Dir.	01	07	13	19
J	17.5	63.5	3.86	1.52	13.8	8.6	E	86	88	59	74
F	18.4	65.2	5.61	2.21	14.7	9.2	E	85	88	57	71
M	20.1	68.2	6.65	2.62	15.4	9.6	SW	83	87	53	68
A	22.7	72.8	6.71	2.64	14.2	8.9	E	85	89	49	66
M	25.2	77.4	9.78	3.85	13.1	8.2	E	84	86	49	66
J	27.1	80.8	22.76	8.96	11.8	7.4	E	88	88	60	75
J	27.9	82.2	23.06	9.08	11.0	6.9	SE	87	87	60	74
A	28.2	82.7	18.75	7.38	11.0	6.9	E	87	88	61	76
S	27.4	81.3	21.59	8.50	12.6	7.9	E	88	90	63	78
O	24.5	76.1	10.39	4.09	13.6	8.5	NE	86	88	59	75
N	20.7	69.2	3.05	1.20	13.3	8.3	NE	86	88	55	74
D	18.3	65.0	3.28	1.29	13.3	8.3	NE	87	89	55	75

ranging from 2,500 m (8,200 ft) in its wider parts down to 160 m (525 ft) in the canal near S-79. Since most of the shoreline of the Caloosahatchee estuary is residential and there is no substantial bank erosion, its plane configuration remains unaltered in time.

The depth of the estuary ranges from 0.3 m (1 ft) at its shallowest points down to 6 m (20 ft) at its deepest points. A narrow navigation channel is maintained at an average depth of approximately 3.5 m (11.5 ft). The overall mean depth of the estuary averages 1.5 m (5 ft) in the section west of Beautiful Island, while the depth at the remaining eastern section is 6.0 m (20 ft). Excluding certain zones of the estuary, especially near heavily populated areas where organic materials in the form of soft mud have accumulated, the rest of the estuarine bottom is fairly stable. A top layer of shell fragments and coarse sand has an armoring effect providing resistance to sediment motion under normal hydrodynamic conditions. Mud near urbanized areas is due to urban runoff and sewage and other plants discharges. A set of characteristic cross sections of the Caloosahatchee estuary, taken from data provided by NOAA, NOS, US Department of Commerce (Nautical Chart 11427) are given respectively in Figure 3, and Appendix A. The locations of the cross sections are given in Figure 4. In order to verify the accuracy of these charts, bathymetry data were collected by District personnel for three different cross sections utilizing the HYDROLAB. The comparison between the collected data and the data from the charts showed very good agreement. Thus, for all practical purposes, the charts suffice for model development.

TIDAL, HYDROLOGIC, AND CLIMATOLOGIC DATA

Tidal Records

The tides in the area are a combination of diurnal and semidiurnal components with an average astronomical tidal range at the river mouth of approximately 0.60 meters (2 ft). Digitized water elevation data exist at six minute time intervals for various sites and for certain periods of time. These specific sites are shown in Figure 3. The tidal characteristics for the different recording locations are inferred by the NOAA Tide Table corrections presented in Table 2. These corrections refer to tidal times and height ratios of the NOAA St. Petersburg primary station. The periods for which data exists for these sites are given in Table 3.

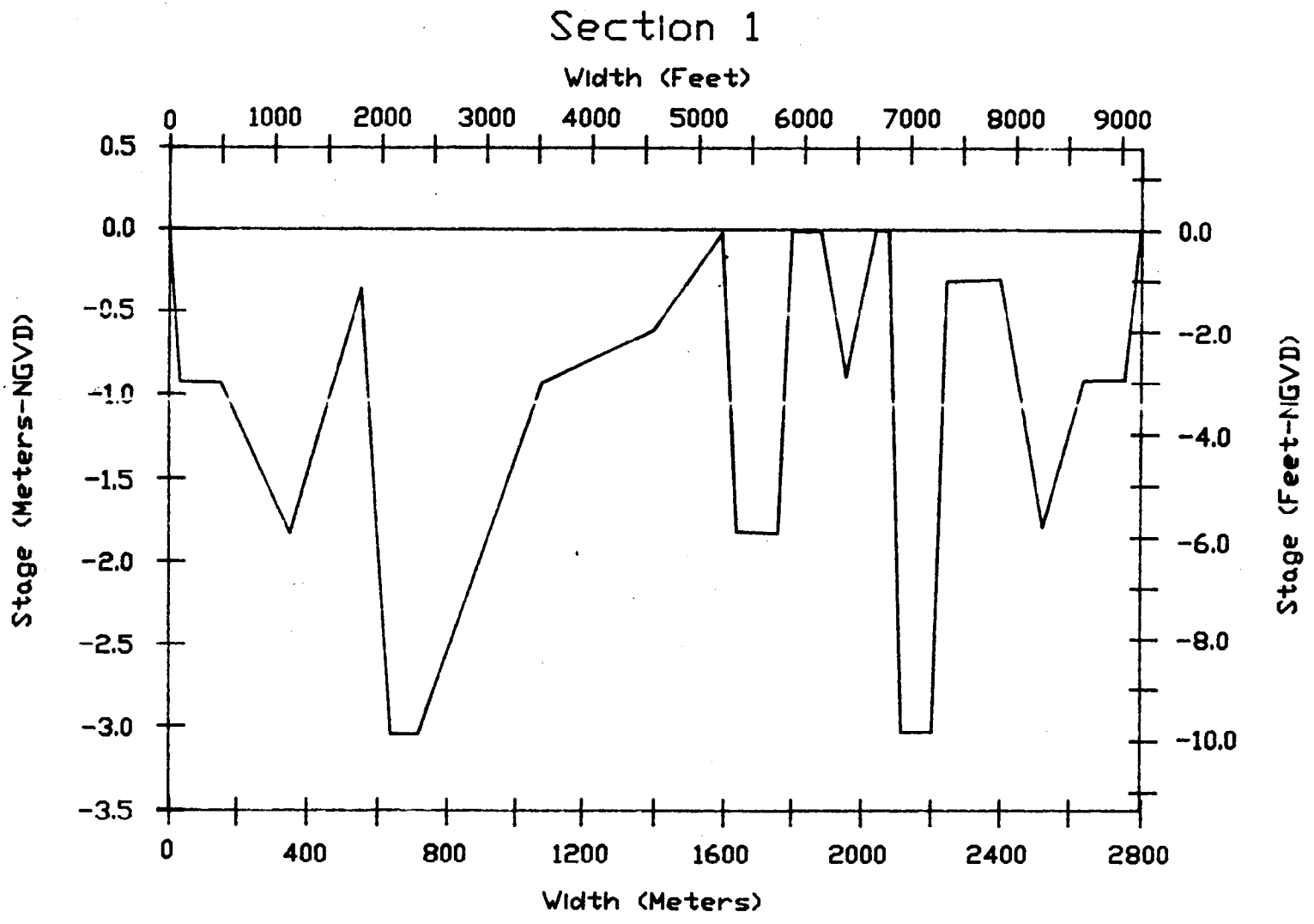

FIGURE 3 Cross-Section of the Caloosahatchee Estuary
NOTE: Remainder of the Cross-sections are located in the Appendix A

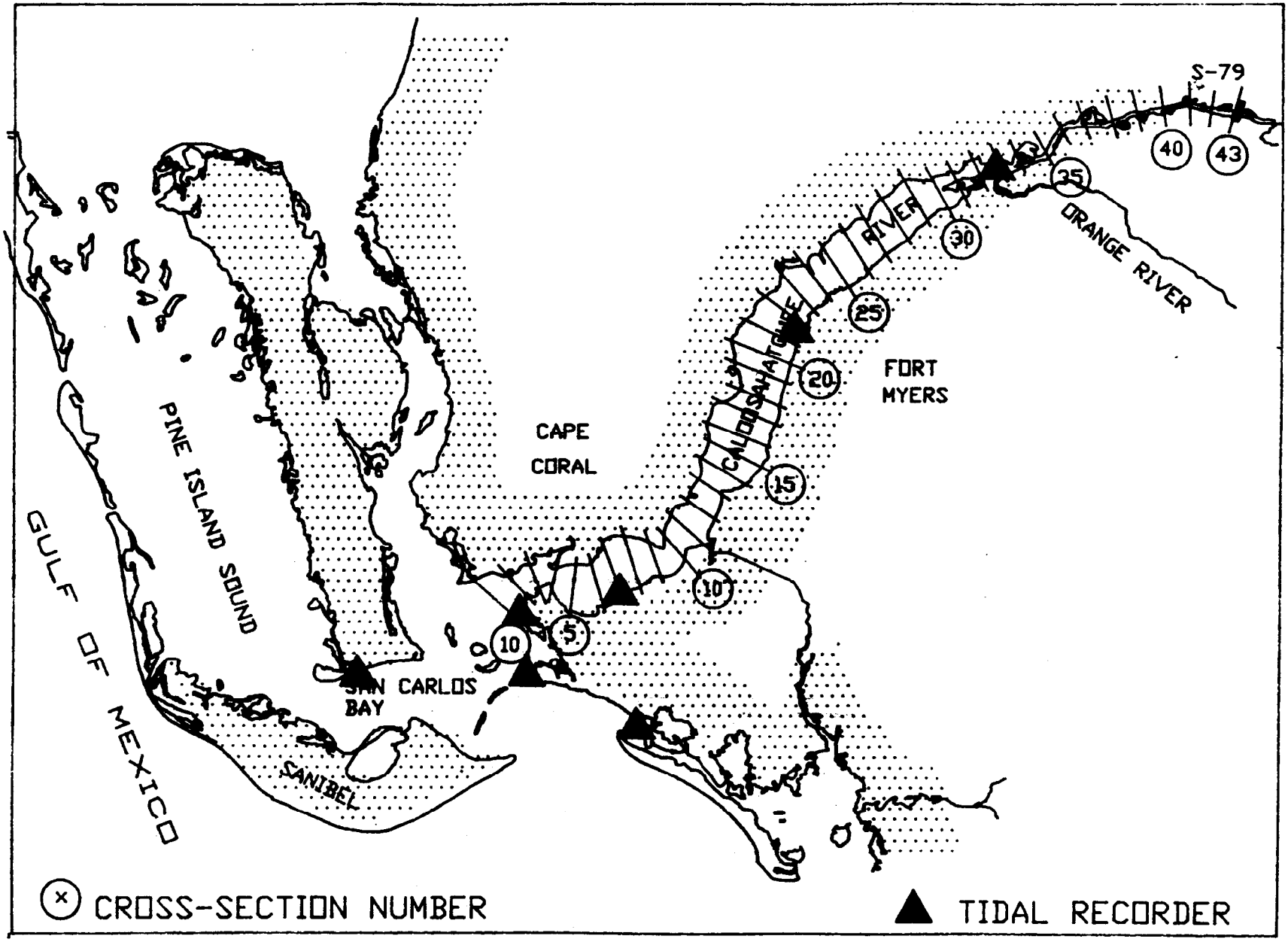

FIGURE 4 Location of Cross-Sections and of Tidal Gauges.

Table 2. Tidal Differences and Other Constants

Location	Differences				Diurnal Range in m./ft.
	Time in Hours and Minutes			Height Ratios	
	H. W.		L. W.	H. W	
Tropical Homesites	-0	08	+0	22	0.87	0.61/2.00
St. James City	-0	30	-0	44	1.04	0.73/2.40
Punta Rassa	-1	01	-1	19	1.04	0.73/2.40
Matanzas Pass	-1	10	-1	34	1.22	0.85/2.80
Cape Coral Bridge	+1	15	+2	02	0.43	0.30/1.00
Iona Shores	+1	08	+1	40	0.43	0.30/1.00
Fort Myers	+2	08	+2	44	0.52	0.37/1.20

NOTE: Heights are referred to mean low water

Regulatory Fresh Water Releases from S-79

S-79 is a reinforced concrete, gated spillway with discharges controlled by eight chain-operated, vertical lift gates and a reinforced concrete lock with two sets of sector gates. The purpose of the structure is to maintain an upstream water stage of 0.914m (3 ft), to pass the design flood (30% of the Standard Project Flood), to restrict downstream flood stages and channel velocities to non-damaging levels, and to prevent salinity intrusion during high tide and low upstream water surface elevations.

The recorded water elevations contain the effects of the astronomical tides as well as other physical inputs such as winds, precipitation, fresh water discharges, evaporation, and ground water flow. The astronomical tides, due to their periodic nature, can be estimated separately using harmonic analysis. The harmonic analysis of tidal data was done under contract by the Department of Oceanography and Ocean Engineering at Florida Institute of Technology (Reichard, 1985). The analysis estimated the variance for the entire input data series, the combined predicted diurnal constituents, the combined semidiurnal constituents, and the residual series. The results, presented in graphical form, provided the collected data, the predicted astronomical tides, the difference between the two, and the residual. A typical example is presented in Figure 5.

The operating criteria of the spillway are as follows:

- The gate opens at a rate of 15.24 cm (6 inches) per minute, with a maximum opening of 3.66 m (12.0 ft.) when the headwater rises to 0.975 m (3.2 feet).
- The gate becomes stationary when the headwater elevation rises or falls to 0.914 m (3.0 feet).
- The gate closes at a rate of 15.24 cm (6 inches) per minute when the headwater elevation falls to 0.853 m (2.8 feet).

Salinity intrusion during lock operations is reduced by two pneumatic barriers installed upstream and downstream of the lock.

Table 3. Period of Tidal Records

Location	Period of Tidal Data	Remarks
Tropical Homesites	02/18/65 - 06/07/66	Data collected
St. James City	10/19/65 - 04/08/71	by the National
Punta Rassa	06/17/77 - 08/04/78	Ocean Service
Matanzas Pass	05/16/73 - 07/09/73	Office of the
Cape Coral Bridge	02/26/65 - 05/26/66	Oceanography
Iona Shores	02/17/65 - 09/30/65	and Marine
Fort Myers	03/08/65 - 03/31/81	Services
Orange River	12/03/84 - 10/14/85	Data by SFWMD

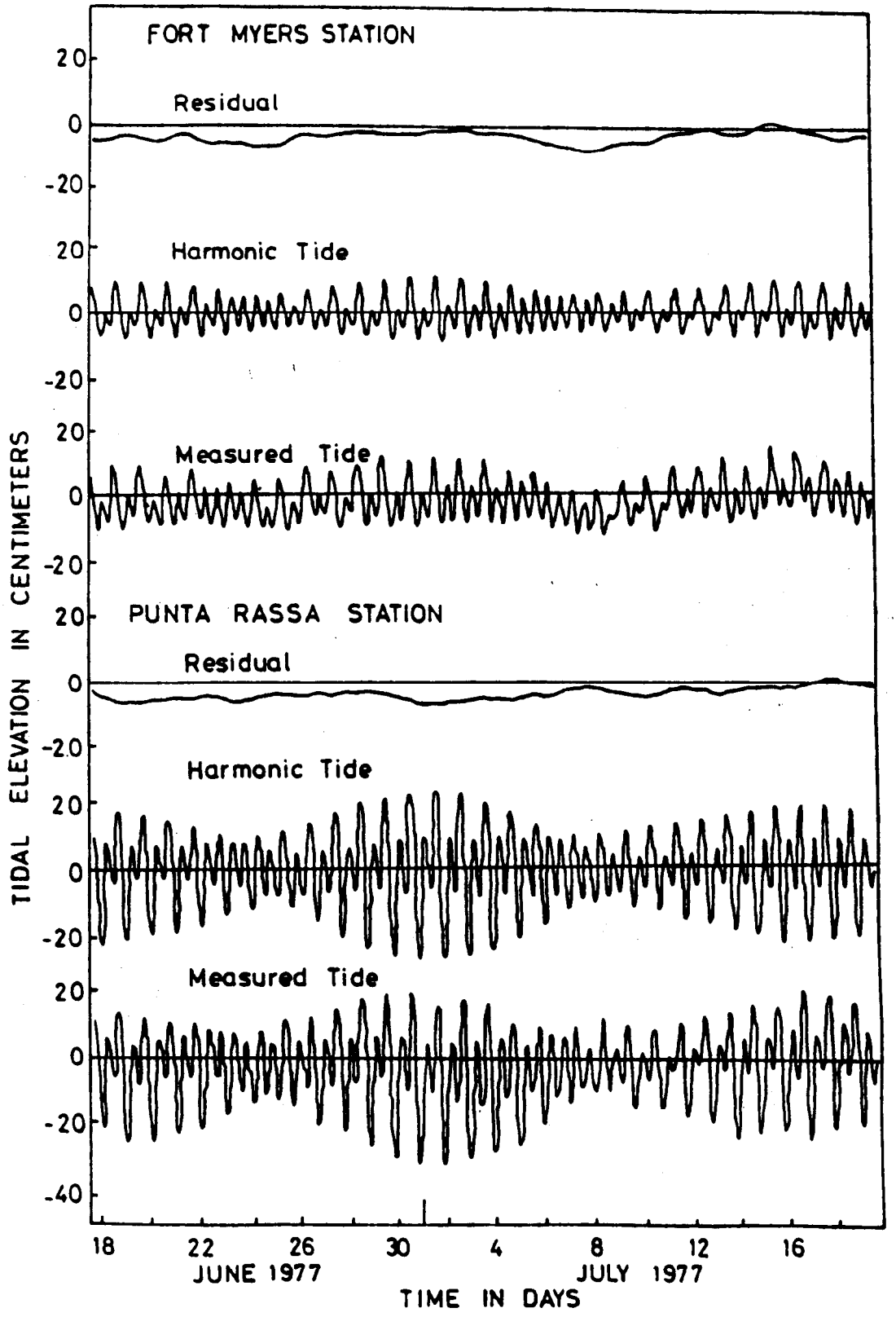

FIGURE 5 Recorded, Astronomical, and Residual Tide

The hydraulic conditions of the structure are recorded by a dual stage recorder, a gate opening recorder, and a gate opening indicator. The discharge is then computed from relations between discharge, hydraulic head, and gate openings. There are records of gage heights from December 1964 to March 1966. From April 1966 to date, there are records of daily average discharges. The data are collected by the US Army Corps of Engineers (COE) and provided by the United States Geological Survey (USGS).

Rainfall Data

There is a large amount of rainfall data from gauges within the adjacent watersheds of the Caloosahatchee River. Those gauges have been operated either by SFWMD, NOAA, or Florida Forestry Service (FFS). The time period that those data were recorded is not the same, but it is scattered along various time intervals. Data are given as daily averages. Figure 6 shows the three drainage basins of the Caloosahatchee estuary and Canal 43. The two drainage basins to the east discharge into the Caloosahatchee estuary through Franklin Dam, while the drainage basin to the west discharges directly to the estuary. The direct discharge is either through tributary flow (e.g. Orange River) or from non-point runoff. A list of the rainfall stations within the western drainage basin is given in Table 4.

A rainfall-runoff relationship for the western drainage basin cannot be established, because of the unavailability of discharge data for the tributaries. The only tributary in the western basin for which rainfall-runoff relationship has been developed is Orange River (Smith, 1955). This relation is given as

$$Y = 37 + 1.55\,X \quad \ldots\ldots\ldots\ldots\ldots \quad [1]$$

where Y = the rainfall in inches and
X = the runoff in inches.

Due to the different land uses between the eastern drainage basins and the western one, direct application of any existing rainfall-runoff relationship for the eastern basins should be used with caution for the Caloosahatchee estuary area. Additional hydrologic information, ground water elevations, and surface water availability for the Caloosahatchee River basin can be found in the studies by Smith (1955), and Fan and Burgess (1983).

Wind and Temperature Data

Information about the winds and temperatures is available from the National Climatic Center (NOAA) for the city of Fort Myers. The data are given at three-hour time intervals, and provide information about wind velocity and direction, air temperature, and other climatological conditions like sky cover, fog, and atmospheric pressure. Data are available from 1949 to present.

Table 4. Period of Rainfall Data Within the Caloosahatchee Estuary Drainage Basins

Station No	Period of available data	Agency
MRF 250	01/11/1968 01/31/1986	SFWMD
MRF 229	05/02/1978 02/28/1985	SFWMD
MRF 5001	12/01/1969 04/30/1986	FFS
MRF 6093	01/01/1909 01/31/1986	USWB
MRF 384	03/01/1984 05/31/1986	SFWMD
MRF 206	01/01/1960 04/30/1986	SFWMD
MRF 235	08/01/1974 04/30/1984	SFWMD
MRF 383	04/01/1984 08/31/1985	SFWMD
MRF 5004	12/01/1969 04/30/1986	FFS
MRF 7093	01/01/1948 11/30/1985	NOAA

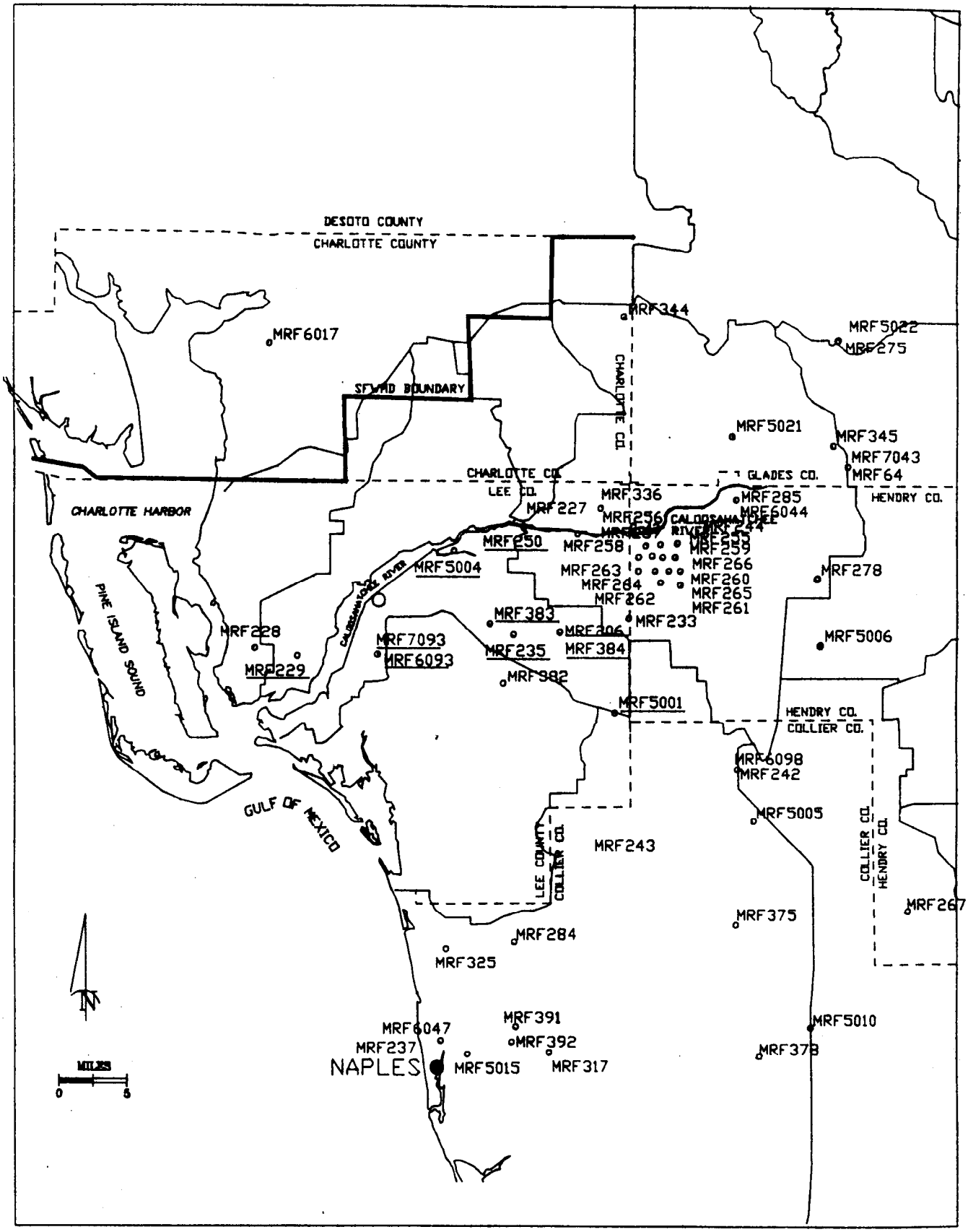

FIGURE 6 Location of the Rainfall Gauges

MATHEMATICAL MODELING OF THE CALOOSAHATCHEE ESTUARY

Conceptual Model

The characteristic geometric features of the Caloosahatchee estuary allow certain simplifications of the system for easier mathematical description. The elongated shape of the estuary allows the use of a one-dimensional longitudinal model, while its shallowness permits a depth-integrated approach. Depending on the objectives, the system can be studied from the near field or far field point of view. In the near field case, emphasis is placed on the local effects of a driving force, while in the far field case large scale or global effects are of interest. Short period wind generated waves, and jet type water discharge from a point source into the estuary can be considered as near field effects, while wind setup, major inflows, and tidal oscillations are far field disturbances.

In this study only the far field features, described by the one-dimensional hydrodynamic equations, are considered.

All estuarine systems are subject to a variety of driving forces such as tides, winds, change in barometric pressure, direct precipitation, surface runoff, evaporation, and ground water seepage. The importance of each of those driving forces may vary in time and space. Evaluation of the importance of those driving forces is not an easy task – the main difficulty stems from their nonlinearity, nonhomogeneity, and time-dependence.

Mathematical models are generally idealizations of real-life complex physical systems. In an initial boundary value problem, such as the estuarine hydrodynamics problem, the solution domain along with the proper initial and boundary conditions must be specified. The initial conditions indicate the state of the system at the beginning of the simulation, while the boundary conditions describe the dependent variables at the boundaries of the system. For periodic phenomena, the initial condition effects tend to dissipate after a few periodic cycles. The boundary conditions are very important because they are solely driving the solution in time, if there are not any "body" forces acting within the solution domain. Common examples of boundary conditions are time histories of water surface elevation, current velocity, or mass flux. Examples of a "body" force are wind stress, bottom stress, and gravity. In an estuary, explicit differentiation between forces acting on the boundary and "body" forces is not possible. However, depending on the situation, certain assumptions can be made so that mathematical modeling is feasible.

Since the water mass of an estuary is relatively small in comparison with the vast water mass of the oceans, the direct attraction of the moon and sun on the estuary can be considered negligible. Thus, the effects of astronomic tides on the estuary are introduced only through the open-sea boundary conditions.

The same is not true for the wind shear stresses. Winds may have both boundary effects through coastal water surface setup and "body" force effects; that is, direct wind stress effects on the water particles within the estuary. The result of the wind stress will be either an increase or a decrease of the magnitude of the water current, depending on whether the wind blows in the same or the opposite direction of the main current. Similarly, boundary and body force effects exist for the case of changes in barometric pressure.

Fresh water discharges, surface runoff, and ground water seepage which affect the mass balance of the system are introduced either through the boundary conditions or as internal source points, depending on the physical system. In this study the physical components incorporated are: tides, fresh water discharges, winds, and surface runoff. Direct precipitation, evaporation, and ground water effects are neglected. The importance of those components cannot be assessed due to lack of data, but is expected to be small on the overall estuarine system.

Governing Equations

The hydrodynamics of the Caloosahatchee estuary can be described mathematically by the one-dimensional, time-dependent, equations of mass conservation and momentum balance, written respectively in their general form as

$$B\frac{\partial h}{\partial t} + \frac{\partial Q}{\partial x} = q_o \qquad \text{[2]}$$

$$\frac{\partial u}{\partial t} + u\frac{\partial u}{\partial x} + g\frac{\partial h}{\partial x} + g|u|u/(C_z^2 H) - gR|w|w/H = 0 \qquad \text{[3]}$$

where

h is the wave height measured from the mean sea level (MSL),

H is the total water depth measured from a reference datum,

u is the current mean velocity,

Q is the water discharge,

B is the width of the channel,

q_o is the unit width inflow (or outflow) discharge,

w is the wind velocity in the longitudinal direction of the estuary,
g is the acceleration of gravity,
C_z is the Chezy coefficient of friction,
R is the wind friction coefficient,
x is the space coordinate, and t is the time.

Equations [2] and [3] constitute a nonlinear, partial differential system of the hyperbolic type that can not be solved analytically in its general form. Solution can be achieved by means of numerical techniques such as the finite differences or finite elements. Furthermore, the numerical solution can be applied either directly to Equations [2] and [3] or after they are written in their characteristic form (Scarlatos, 1981; McDowell and O'Connor, 1977). The assumptions under which the system of Equations [2] and [3] is valid are the following:

(a) The curvature of the free surface is very small so that the hydraulic pressure distribution is hydrostatic,
(b) The energy losses in unsteady flow are the same with the energy losses in steady flow,
(c) The actual velocity profile along the depth does not affect the wave propagation,
(d) The bottom slope is very small,
(e) The fluid is incompressible and homogeneous.

Since the system is tide-dominated, the initial conditions are not essential. Starting with a state of equilibrium, i.e., a quasi-steady state can be reached after few tidal cycles. The boundary conditions are specified by the water surface elevation at Shell Point and the water velocity at S-79, i.e.,

$$u(x,0) = h(x,0) = 0 \quad \cdots\cdots [4]$$

$$h(0,t) = F(t) \quad \cdots\cdots [5]$$

$$u(l,t) = G(t) \quad \cdots\cdots [6]$$

where l is the total length of the estuary. Therefore, the boundary conditions are of the Dirichlet type, since the value of the variable is directly specified at the boundary.

Regarding the longitudinal salinity distribution, a one-dimensional, time-dependent, advective-dispersive model can be written as

$$\frac{\partial S}{\partial t} + u(x,t)\frac{\partial S}{\partial x} - \frac{\partial}{\partial x}\left[D(x,t)\frac{\partial S}{\partial x}\right] = 0 \quad \cdots\cdots [7]$$

where S(x,t) is the salinity concentration and D(x,t) is the longitudinal dispersion coefficient. The initial and boundary conditions for the salinity distribution can be assumed as

$$S(x,0) = S_0(1 - x/l) \quad \cdots\cdots [8]$$

$$S(0,t) = S_0 \quad \cdots\cdots [9]$$

$$\frac{\partial S(l,t)}{\partial x} = 0 \quad \cdots\cdots [10]$$

Equation [8] indicates that initially there is a linear distribution of salinity along the estuary, while Equations [9] and [10] assume a constant salinity S_0 at the river mouth and no-flux conditions at S-79, respectively.

Harmonic Approximation of the Hydrodynamic Equations

By neglecting the nonlinear convective term, inflow discharge, and wind effects, Eqs. [2] and [3] can be combined in the form of Telegrapher's equation, i.e.

$$c_0^2\frac{\partial^2 h}{\partial x^2} = \frac{\partial^2 h}{\partial t^2} + gM\frac{\partial h}{\partial t} \quad \cdots\cdots [11]$$

or

$$c_0^2\frac{\partial^2 u}{\partial x^2} = \frac{\partial^2 u}{\partial t^2} + gM\frac{\partial u}{\partial t} \quad \cdots\cdots [12]$$

where c_0 is the wave phase velocity ($c_0 = (gH)^{1/2}$), and M is the linearized friction factor given as

$$M = \left(\frac{f}{g}\right)\tan 2\alpha \quad \cdots\cdots [13]$$

where f is the tidal frequency ($f = 2\pi/T$), and α is the phase difference between the tidal wave and tidal current due to the bottom friction effects. The tidal period is denoted by T.

If total reflection is assumed at Structure 79, i.e. u (l,t) = 0, then the solution of Eq. [7] is given as

$$h = a_0[\exp(-mx)\cos(ft - kx) + \exp(mx)\cos(ft + kx)] \quad \cdots\cdots [14]$$

where a_0 is half the wave amplitude at the reflecting boundary, m is the friction damping coefficient, and k is the wave number related to the wave length L as

$$k = 2\pi/L \quad \text{[15]}$$

Accordingly, the velocities are given as

$$u = a_o c_o k_o \{exp(-mx)\cos(ft - kx + a) - exp(mx)$$

$$\cos(ft + kx + a)\}/H(m^2 + k^2)^{\frac{1}{2}} \quad \text{[16]}$$

where k_0 is the nonfrictional wave number defined as

$$k_0 = (k^2 - m^2)^{\frac{1}{2}} \quad \text{[17]}$$

Utilization of Eqs. [11] and [12] requires knowledge of the damping coefficient m and the wave number k. Estimation of those parameters can be done by using the methodology proposed by Ippen and Harleman (Ippen, 1966). The methodology is semi-empirical and based on a nomograph given by Figure 7. The coordinates of the nomograph are respectively the normalized maximum wave height h_H/ h_{oH} and the time shift of the occurrence of the maximum wave height h_H, with respect to the closed-end ft_H, where h_{oH} is the maximum wave height at the closed-end boundary (Franklin dam).

Data are plotted on the nomograph of Figure 7, and a curve Φ is chosen. From the same nomograph the wave number k can be estimated since the distance x is known. Then, the damping coefficient m can be derived from the following relation

$$m = \{\phi/(2\pi)\}k \quad \text{[18]}$$

Equations [11] and [12] can be used to provide rough estimates of the velocities (Eq. 12) and wave heights (Eq. 11) for preliminary studies. Therefore, they can be used as initial conditions, instead of using $u = h = 0$, so that quasi-steady conditions can be established faster.

Leap-Frog Explicit Finite Differences Scheme

A more generalized solution of the system of Eqs. [2] and [3] can be derived by writing the equations in a finite difference form. For that purpose the system is discretized into a finite number of points where the dependent variables h(x,t) and u(x,t) are evaluated. The partial derivatives are expanded in a truncated Taylor series and substituted accordingly into the original equations (Ames, 1977). There are many different ways that the finite difference approximation of the governing equations can be achieved. For this study the leap-frog explicit scheme was chosen for its simplicity and efficiency (McDowell and O'Connor, 1977). According to that scheme the governing equations (Eqs. 2 and 3) are written as follows

$$B_{i+1}(h^j_{i+1} - h^{j-2}_{i+1})/\Delta t + (Q^{j-1}_{i+2} - Q^{j-1}_{i})/\Delta x - q^j_{0i} +$$

$$O(\Delta x^2, \Delta t^2) = 0 \quad \text{[19]}$$

$$(u^{j+1}_i - u^{j-1}_i)/\Delta t + u^j_i(u^j_{i+1} - u^j_{i-1})/\Delta x +$$

$$g(h^j_{i+1} - h^j_i)/\Delta x + g\,u^j_i|u^j_i|/(C^2_{zi} H^j_i)$$

$$- gRW^j_i|W^j_i|/H^j_i + O(\Delta x^2, \Delta t^2) = 0 \quad \text{[20]}$$

where the superscripts j denote time steps, and the subscripts i nodes in space. The function O() indicates the order of accuracy of the numerical approximation with respect to time and space step. Equations [19] and [20] are of second order. The nonlinear convective acceleration terms in Eq. [20] are linearized by writing the velocities u^j_i, u^j_{i+1}, u^j_{i-1} according to the following relations

$$u^j_i = (u^{j+1}_i + u^{j-1}_i)/2 \quad \text{[21]}$$

$$u^j_{i+1} = (u^{j-1}_{i+2} + u^{j+1}_i)/2 \quad \text{[22]}$$

$$u^j_{i-1} = (u^{j+1}_i + u^{j-1}_{i-2})/2 \quad \text{[23]}$$

Therefore, the convective term becomes

$$u^j_i(u^j_{i+1} - u^j_{i-1})/\Delta x = (u^{j+1}_i + u^{j-1}_i)$$

$$(u^{j-1}_{i+2} - u^{j-1}_{i-2})/(4\Delta x) + O(\Delta t) \quad \text{[24]}$$

Similarly the bottom friction loss term is linearized as

$$g\,u^j_i|u^j_i|/(C^2_{zi} H^j_i) = g\,u^{j+1}_i|u^{j-1}_i|/(C^2_{zi} H^j_i))$$

$$+ O(\Delta t) \quad \text{[25]}$$

As can be seen, the linearization of the convective and bottom friction terms reduces the accuracy of the numerical scheme to that of the first order. Considering a prismatic channel, and after substitution of the linearized approximations, the dependent variables h(x,t) and u(x,t) can be estimated as follows

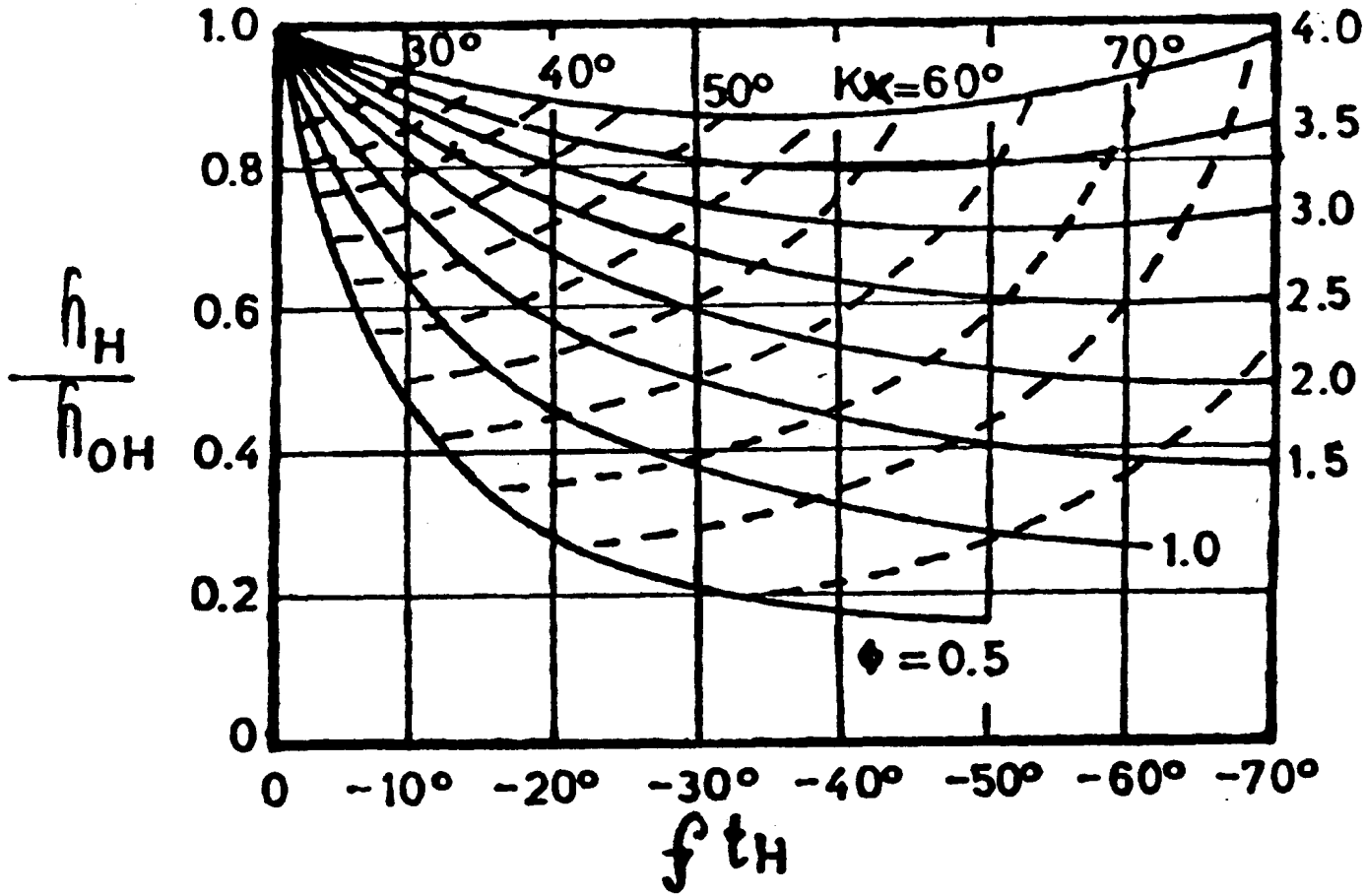

FIGURE 7 Harmonic Analysis, Φ - kx Nomograph

$$h_{i+1}^{j} = h_{i+1}^{j-2} - [B_{i+2}(uH)_{i+2}^{j-1} - B_i(uH)_i^{j-1}]\Delta t/$$

$$(B_{i+1}\Delta x) + q_{0i}^{j}\Delta t/B_{i+1}) \quad \ldots\ldots\ldots\ldots \quad [26]$$

and

$$u_i^{j+1} = [u_i^{j-1}/\Delta t - u_i^{j-1}(u_{i+2}^{j-1} - u_{i-2}^{j-1})/(4\Delta x) -$$

$$g(h_{i+1}^{j} - h_{i-1}^{j})/\Delta x + gRW_i^j|W_i^j|/H_i^j]/[1/\Delta t + (u_{i+2}^{j-1} -$$

$$u_{i-2}^{j-1})/(4\Delta x) + g|u_i^{j-1}|/(C_{zi}^2 H_i^j)] = 0 \quad \ldots\ldots\ldots \quad [27]$$

If the initial and boundary conditions are known, (Figure 8), then Eq. [26] can be utilized for estimation of the wave height h(x,t) at points (i + 1, j), where i = 1, 3, 5, 7, ..., etc., and j = 1. This requires an iterative process because the quantity H^{j+1}_{i+2} depends upon the value of the wave height at point (i + 1, j). Thus, initially H^{j+1}_{i+2} is estimated as the average between the values at points (i + 1, j-1) and (i + 3, j-2), and then as the average between the points (i + 1, j) and (i + 3, j-2). Once the wave heights have been estimated at time level j, then the current velocities can be calculated from Eq. [27] at points i during time j + 1. The value of u^{j+1}_{-1} is obtained by extrapolation of the values of u(x,t) at points (1, j + 1) and (3, j + 1). Also, the water depth H(x,t) at points (i,j) is taken as the average of the water depth at points(i - 1,j) and (i + 1,j). A schematic representation of the x - t solution domain is given at Figure 8. From that figure it can be seen that the wave heights are computed at even-numbered nodal points and half time steps, while the current velocities are computed at odd-numbered nodal points and full time steps. This is the reason that the scheme is referred to as leap-frog.

Since the numerical scheme is explicit, for numerical stability, compliance with the Courant-Friedrich-Levy criterion is required, i.e.,

$$\Delta x/\Delta t > c \pm u \quad \ldots\ldots\ldots\ldots\ldots\ldots \quad [28]$$

where c is the phase velocity of the traveling wave.

Crank-Nicholson Implicit Finite Difference Scheme

The numerical solution of the time dependent salinity distribution equation, Eq. [7], is based on the implicit Crank-Nicholson finite differences scheme. After discretization, the governing equation reads

$$(S_i^{j+1} - S_i^j)/\Delta t + u_i^j(S_{i+1}^{j+1} - S_{i-1}^{j+1} + S_{i+1}^j$$

$$- S_{i-1}^j)/(4\Delta x) - D_i(S_{i+1}^{j+1} - 2S_i^{j+1} + S_{i-1}^{j+1}$$

$$+ S_{i+1}^j - 2S_i^j + S_{i-1}^j)/(2\Delta x^2) = 0 \quad \ldots\ldots\ldots\ldots \quad [29]$$

Rearranging Eq. [29] with respect to the unknowns it yields

$$[-u_i^{j+1}/(4\Delta x) - D_i/(2\Delta x^2)]S_{i-1}^{j+1} + (1/\Delta t + D_i/\Delta x^2)S_i^{j+1}$$

$$+ [u_i^{j+1}/(4\Delta x) - D_i/(2\Delta x^2)]S_{i+1}^{j+1} = [u_i^{j+1}/(4\Delta x) +$$

$$D_i/(2\Delta x^2)]S_{i-1}^j + (1/\Delta t - D_i/\Delta x^2)S_i^j + [-u_i^{j+i}/(4\Delta x) -$$

$$D_i/(2\Delta x^2)]S_{i+1}^j \quad \ldots\ldots\ldots\ldots\ldots\ldots \quad [30]$$

Equation [30] constitutes a linear algebraic system with a tridiagonal matrix. Therefore, the system can be solved directly, without iterations, by using the Thomas algorithm [Ames, 1977]. The sequence of solution for the entire program is as follows:

(a) Wave heights are estimated at half-time step and even-numbered nodes from Eq. [26],
(b) Current velocities are estimated at full-time step and odd-numbered nodes from Eq. [27].
(c) Salinity concentration is estimated at full time step at all points from Eq. [30].

DATA ANALYSIS

Assessment of the effects of the various physical components such as tides, fresh water discharges, winds, rainfall-runoff, ground water seepage, and evapotranspiration on the estuarine system requires a synoptic set of field data. The data must cover both the spatial and temporal extent of the system under study, and must provide information for every major physical component. Negligence of any particular controlling force may lead to inaccuracies and incorrect conclusions. In many cases however, experience and intuition suffice to predict the response of the system

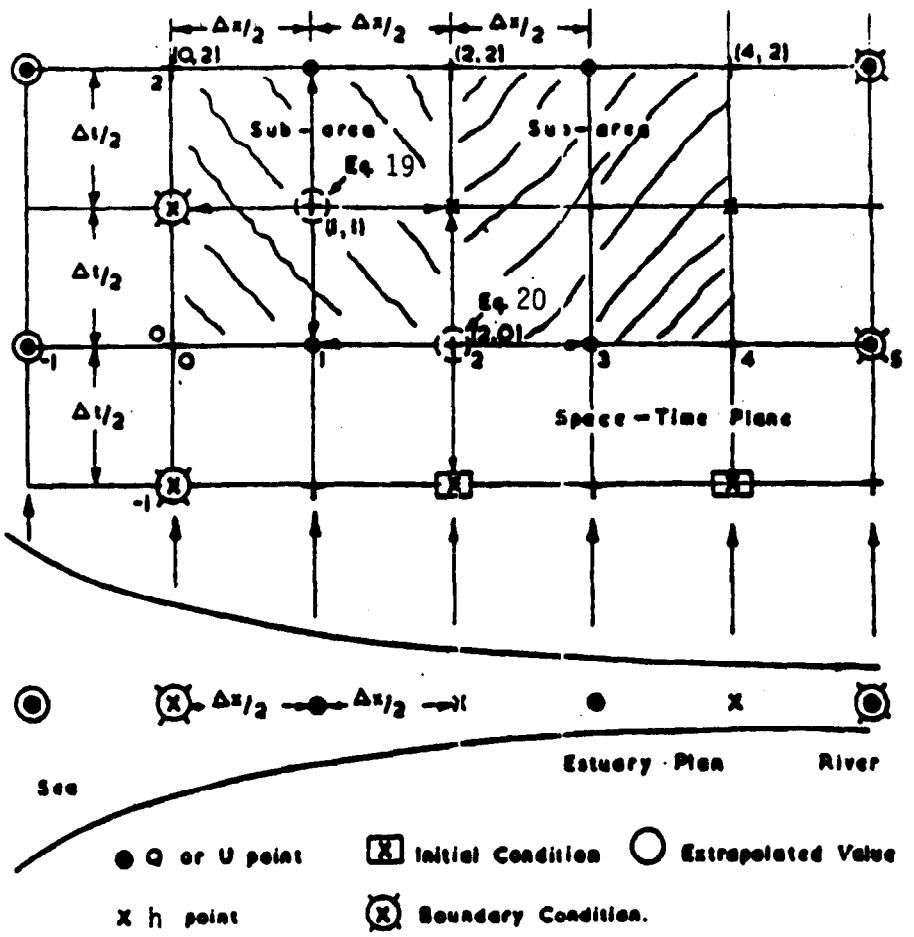

FIGURE 8 Schematic Representation of the Finite Differences Network

qualitatively. For example, it is reasonable to expect the winds to cause a setup of the water surface, the discharges to increase downstream velocities, and the evapotranspiration to deplete the water mass. Since the most easily observed quantity is the water elevation, the impact on the hydrodynamics is usually assessed in terms of water levels. The recorded water levels, however, show the combined effect of all the physical causes. In order to separate the astronomical tide from the residual, harmonic analysis is required. The harmonic analysis represents the tide in the series form of Equation 31.

$$H = H_o + \Sigma_n f_n a_n \cos[r_n t - (v_o + U)_n - k_n] \quad \ldots\ldots \quad [31]$$

where H_0 is the mean water level from the reference datum, f_n is a factor for reducing the mean amplitude a_n of the component n to the year of the data, r_n is the speed of the component, $(v_0 + U)_n$ is the value of equilibrium argument of component n for the period of observation when t is zero, t is the time referred to the beginning of the epoch (specific 19-year period), and k_n is the local epoch of component n (Schureman, 1958). Equation [31] can be simplified as

$$H = H_o + \Sigma_n A_n \cos[2\pi t/T_n + S_n] \quad \ldots\ldots\ldots \quad [32]$$

where A_n is the wave amplitude of the particular harmonic constituent, T_n is the period of the nth tidal constituent, and s_n is the corresponding phase difference. Harmonic analysis of the tidal records at the stations given in Table 5 indicate that the predominant tidal components are the semidiurnal M_2 component, and the diurnal components O_1 and K_1 (Reichard, 1985). The effects of the semidiurnal components S_2 and N_2 are minimal, while all the other components can be completely neglected. Those different tidal components are the result of differential attraction of the vast ocean water mass by various celestial bodies.

In Figures 9 and 10, the recorded water elevation data have been separated into the harmonic tide and the residual tide. In addition, rainfall, wind direction and velocity, and discharge from the Franklin dam are plotted respectively for the months of February ("dry" season) and August ("wet" season) of 1974. The conclusions that can be drawn from those figures are: (a) during "dry" season the residual tide is much less than the residual of the "wet" period. Western winds on February 8, 1974, caused amplification of the water surface by pushing the water upstream. On the contrary, on February 27 and 28, 1974, eastern winds depressed the water surface by pushing the water toward the Gulf. Eastern winds caused surface depression also during the period of August 22 to 24, 1974. A peak, due to rainfall, appeared on the residual tide on February 20, 1974. The only available rainfall-runoff relationship for the Caloosahatchee estuary area is the one developed for the Orange River (Eq. 1). Analysis of the data provided a direct average monthly runoff from Orange River taken as a percentage of the average annual runoff (Smith, 1955). Those data are presented in Figure 11. Additional causes like evapotranspiration, ground water seepage, and effects of

Table 5. Amplitude and Phase Shift of the Major Tidal Components

Location	Tidal Constituent					
	M_2		O_1		K_1	
	A_n [m]	s_n	A_n [m]	s_n	A_n [m]	s_n
Tropical Homesites	0.16	78°	0.11	60°	0.10	275°
St. James City	0.19	247°	0.13	173°	0.12	318°
Punta Rassa	0.23	39°	0.09	321°	0.13	333°
Matanzas Pass	0.25	340°	0.13	60°	0.18	155°
Cape Coral Bridge	0.07	150°	0.07	276°	0.06	175°
Iona Shores	0.19	35°	0.06	21°	0.07	322°
Fort Myers	0.09	341°	0.08	294°	0.08	344°
Orange River	0.09	357°	0.07	67°	0.10	207°

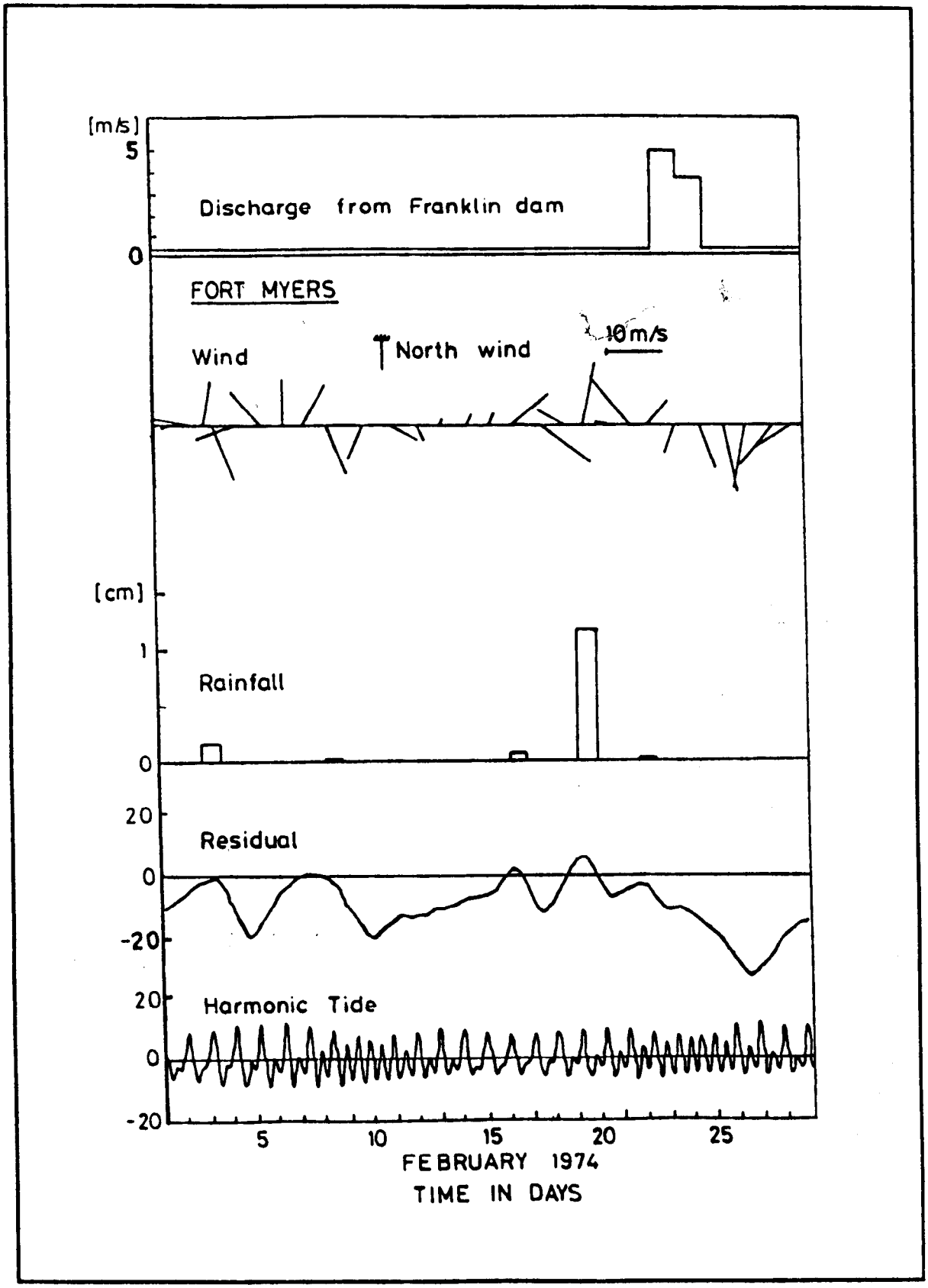

FIGURE 9 Hydrologic characteristics during a "dry" month

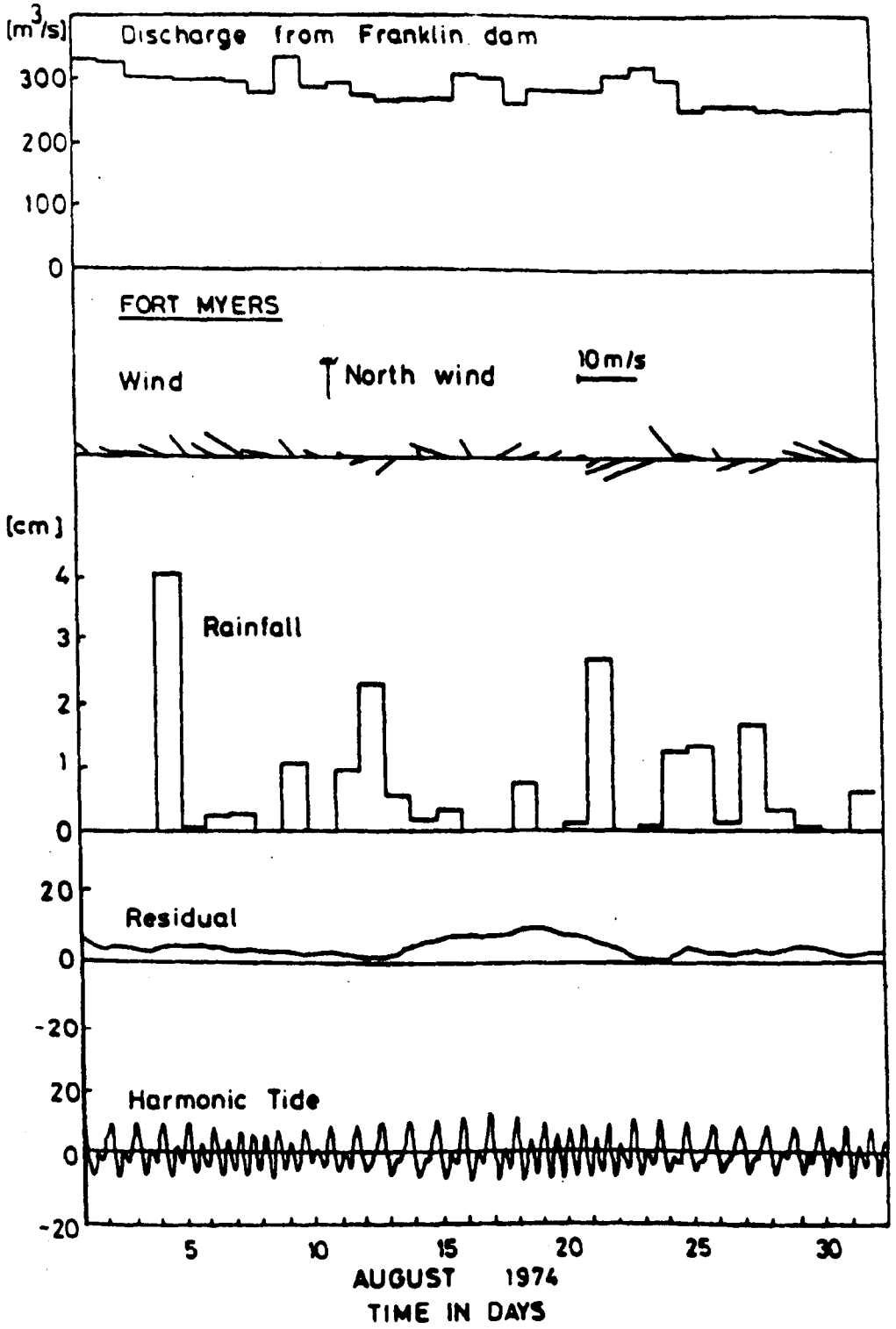

FIGURE 10 Hydrologic characteristics during a "wet" month

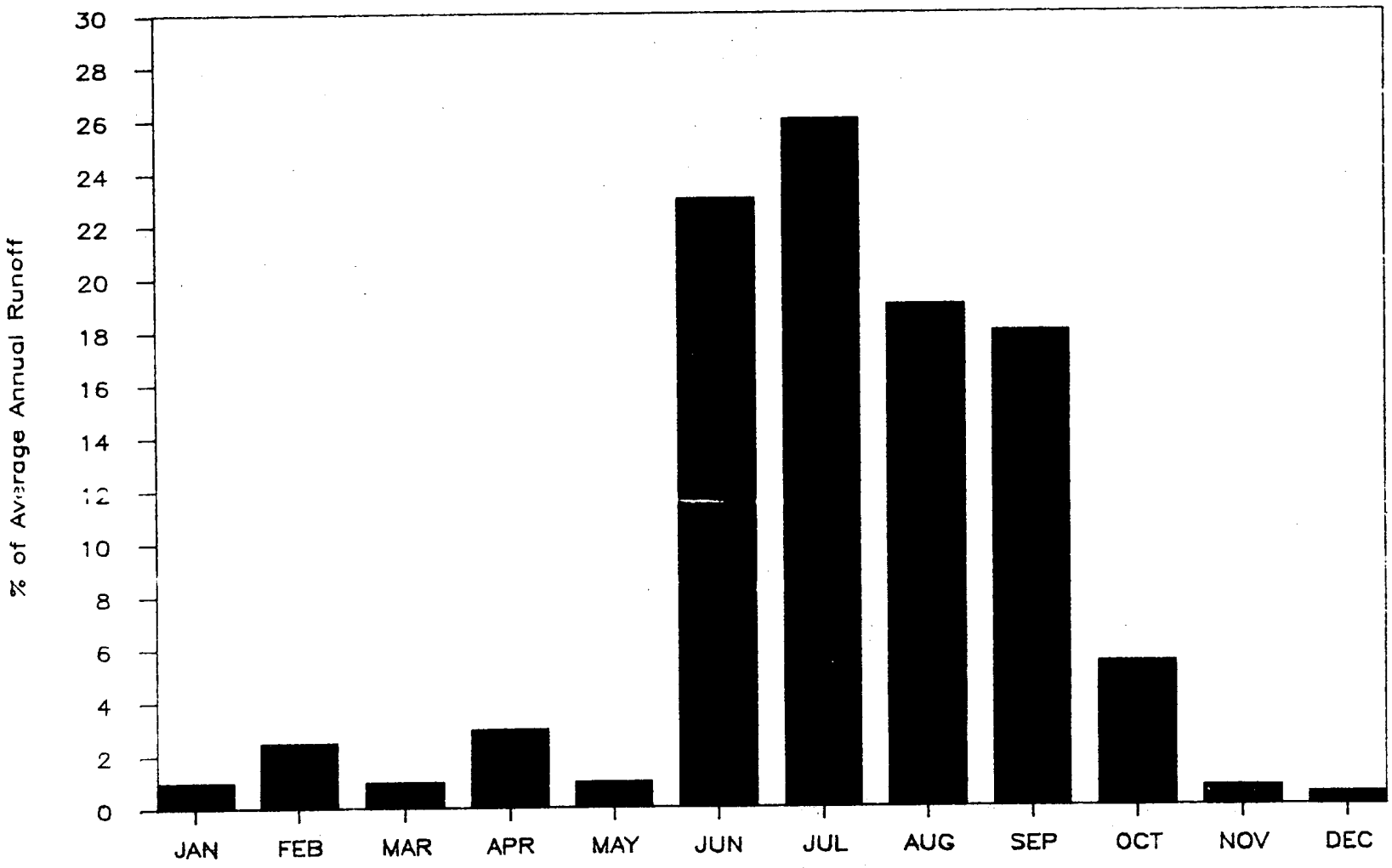

FIGURE 11 Average Monthly Runoff of Orange River

hydrologic events occuring in other adjacent areas may influence the water elevation. However, the implicit and nonlinear character of the phenomenon prohibits a direct quantitative estimation of those effects. Generally, the residual tide is an indication of the overall mass balance and dynamic contribution of all physical components but the astronomic tide.

MODEL APPLICATION

Input Data

For computational purposes the estuary was discretized into 42 segments – each one of approximately 1 km (0.622 miles) in length. The cross sections were taken from the data given in Figure 4. Since the shape of the cross sections is irregular, an equivalent depth was utilized, defined as the ratio of the cross section area over the surface width. The area and the equivalent depth for the various cross sections are given in Table 6. Then, for each segment, a mean depth and a mean width was estimated by taking the arithmetic average of the equivalent depth and the surface width of the two cross sections at the ends of the specific segment. The boundary conditions were defined by an harmonic disturbance at the sea entrance of the estuary, and by the fresh water discharge at Franklin dam.

The astronomical tide is described by its three main harmonic constituents, i.e. M_2, O_1, and K_1. An average tidal amplitude and phase shift for each component is assumed, based on the data given at the recording sites close to the estuarine mouth. The periods were taken as 12.42, 25.82, and 23.93 hours for the M_2, O_1, and K_1 constituents respectively.

Runoff effects can be incorporated by specifying inflow disharges at various nodal points. The only direct rainfall-runoff relation included in the model is the Orange River. This option is accomodated by specifying the month of the year so that the runoff is estimated as a percentage of the annual runoff according to Figure 11. Assuming an average annual rainfall of 125 cm (50 in), from Eq. 1, the annual runoff is 21 cm (8.4 in). An estimation of the annual runoff volume can be obtained by multiplying the average annual runoff by the drainage area. The drainage area of the Orange River is approximately 215 km^2 (83.4 sq. mi.); thus, the annual runoff volume is about 4.5×10^7 m^3 (1.589×10^9 ft^3) Based on that estimation, and on the percentages of Figure 11, an average discharge for each month is presented in Table 7.

The initial conditions can be either an equilibrium state ($h=0$, $u=0$), or data obtained from the application of the harmonic analysis approach. In the former case, the model has to run for at least five tidal cycles so that the quasi-steady state periodic

Table 6. Cross Section Areas and Equivalent Depths

No.	Area [m^2/ft^2]	Depth [m/ft]	No.	Area [m^2/ft^2]	Depth [m/ft]	No.	Area [m^2/ft^2]	Depth [m/ft]
1	3221/34670	1.15/3.77	2	817/8794	0.73/2.45	3	1561/16802	1.45/4.75
4	2983/32109	2.26/7.41	5	4416/47533	1.97/6.46	6	4459/47996	2.19/7.19
7	3800/40902	1.46/4.79	8	3690/39718	1.68/5.51	9	2232/24025	1.51/4.95
10	1915/20612	1.65/5.41	11	3636/39138	1.89/6.20	12	2738/29471	1.80/5.91
13	3117/33551	2.44/8.01	14	4014/43206	1.65/5.41	15	4154/44713	1.48/4.86
16	4111/44250	1.43/4.60	17	3916/42151	1.63/5.34	18	3386/36447	1.69/5.54
19	3910/42086	1.58/5.18	20	4294/46220	1.53/5.02	21	3605/38803	1.48/4.86
22	3666/39460	1.55/5.09	23	3343/35983	1.49/4.83	24	2721/29289	1.89/6.20
25	2715/29224	1.23/4.04	26	2495/26856	1.04/3.41	27	2379/25607	1.08/3.54
28	2489/26791	1.13/3.71	29	2166/23315	1.08/3.54	30	1836/19762	0.92/3.02
31	1525/16415	0.95/3.12	32	854/9192	0.71/2.33	33	695/7480	0.83/2.72
34	750/8072	1.10/3.61	35	1397/15037	1.52/4.99	36	628/6759	2.24/7.35
37	780/8396	2.79/9.15	38	781/8407	2.79/9.15	39	732/7879	0.83/2.72
40	756/8138	4.73/15.52	41	756/8183	4.73/15.51	42	7568183	4.73/15.52
43	756/8138	4.73/15.52						

Table 7. Average Discharge from Orange River

Month Discharge [m3/s]/[cfs]	Month Discharge [m3/m/s]/[cfs/ft/s]	Month Discharge [m3/m/s]/[cfs/ft/s]
Jan. 0.143/0.5039	Feb. 0.0357/1.2597	March 0.0143/0.5039
Apr. 0.0428/1.5116	May 0.0143/0.5039	June 0.3282/11.5890
July 0.3710/13.1006	Aug. 0.2640/9.3216	Sept. 0.2500/8.8177
Oct. 0.0714/2.5194	Nov. 0.0143/0.5039	Dec. 0.0071/0.2519

conditions can be established, while in the latter case those conditions are established much faster.

The values of Chezy's coefficient of friction C_z can be different at each segment, but must remain constant in time. A constant value of $C_z = 60$ $m^{1/2}/s$ (108.66 $ft^{1/2}/s$) was assumed. The dispersion coefficient D was assumed constant and equal to 800 m^2/s (8611 ft^2/s), for the entire estuary. The wind velocity w and the wind friction coefficient R, are assumed as constants in both space and time for the duration that wind effects are considered. The wind friction coefficient is assumed as equal to 0.1×10^{-5} s^2/m ($0.328 \times 10^{-5} S^2/ft$). The values of these constants were taken from the literature and not from actual calibration.

The times of initiation and termination of the fresh water/runoff disharges and of the wind effects are provided apriori. The space and time step have to be specified, but attention must be placed so that the Courant-Friedrich-Lewy criterion (Eq. 28) is satisfied. A space step of 1000 m (3280 ft) and a time step of 60 seconds were used in this study. The results are provided in digital form in terms of water elevation, mean water velocity, and salinity concentration at nodal points for every time step.

The model has the option of simulating either the hydrodynamics of the estuary, or both hydrodynamics and salinity distribution.

Model Calibration and Verification

In order to assess the accuracy of the hydrodynamic model EDASM-B (Estuarine Dynamics And Salinity Model - BASIC) under controlled conditions, the model was tested against laboratory data available from Waterways Experiment Station, US Army, COE (Ippen, 1966). The data were taken from an experimental channel 99.67 m (327 ft) long, 0.23 m (0.75 ft) wide, and 0.152 m (0.5 ft) deep. A tidal oscillation was generated at one end of the channel with an amplitude of 0.0152 m (0.05 ft) and a period of 600 seconds. The roughness consisted of 0.635 cm (1/4 in.) square strips attached at the sides of the channel, which created an estimated Chezy's coefficient of friction equal to 36 $m^{1/2}/s$ (65.20 $ft^{1/2}/s$) The results between laboratory data and simulation output by the leap-frog numerical model, for a station at the mid-point of the channel are represented in Figure 12. Agreement between the data is satisfactory.

The salinity part of the model was tested against closed-form solutions. Assuming constant velocity U and constant dispersion coefficient D, the solution of Eq. 7 when $C(0,t) = C_o$ = constant, and $C(\infty,t) = 0$, $C(x,0) = 0$, is given as (Ippen, 1966)

$$C/C_o = 0.5\, exp(Ux/D)\, erfc\{[x + Ut]/[2(Dt)^{1/2}]\} + 0.5\, erfc\{|x - ct|/[2(Dt)^{1/2}]\} \quad \text{[33]}$$

where the complementary error function erfc(y) = 1-erf(y) and

$$erf(y) = [2/(m)^{1/2}] \int_o^y exp(-r^2)\, dr \quad \text{[34]}$$

where r is a dummy variable. For the hypothetical case of U = 0.5m/s, D = 800 m^2/s (8611 ft^2/s), and C_o = 1, the comparison, and good agreement, between closed-form solution (Eq. 33) and the model EDASM-B are represented in Figure 13. Due to the lack of a synoptic set of data, a limited test of the hydrodynamic part of the EDASM-B model was conducted for the prevailing hydrologic conditions of October 30, 1975. The data utilized are those described in the preceding section of Input Data. The results given in the form of surface elevations at three locations: estuarine entrance, Fort Myers, and Franklin Dam, are represented in Figure 14. From this Figure it is obvious that the model simulates adequately the hydrodynamics of the Caloosahatchee estuary. The salinity part was not tested against actual data within the estuary. A follow-up report will assess the salinity distribution within the Caloosahatchee estuary and provide guidelines for gate operations at S-79, which will comply to ecologically acceptable salinity levels.

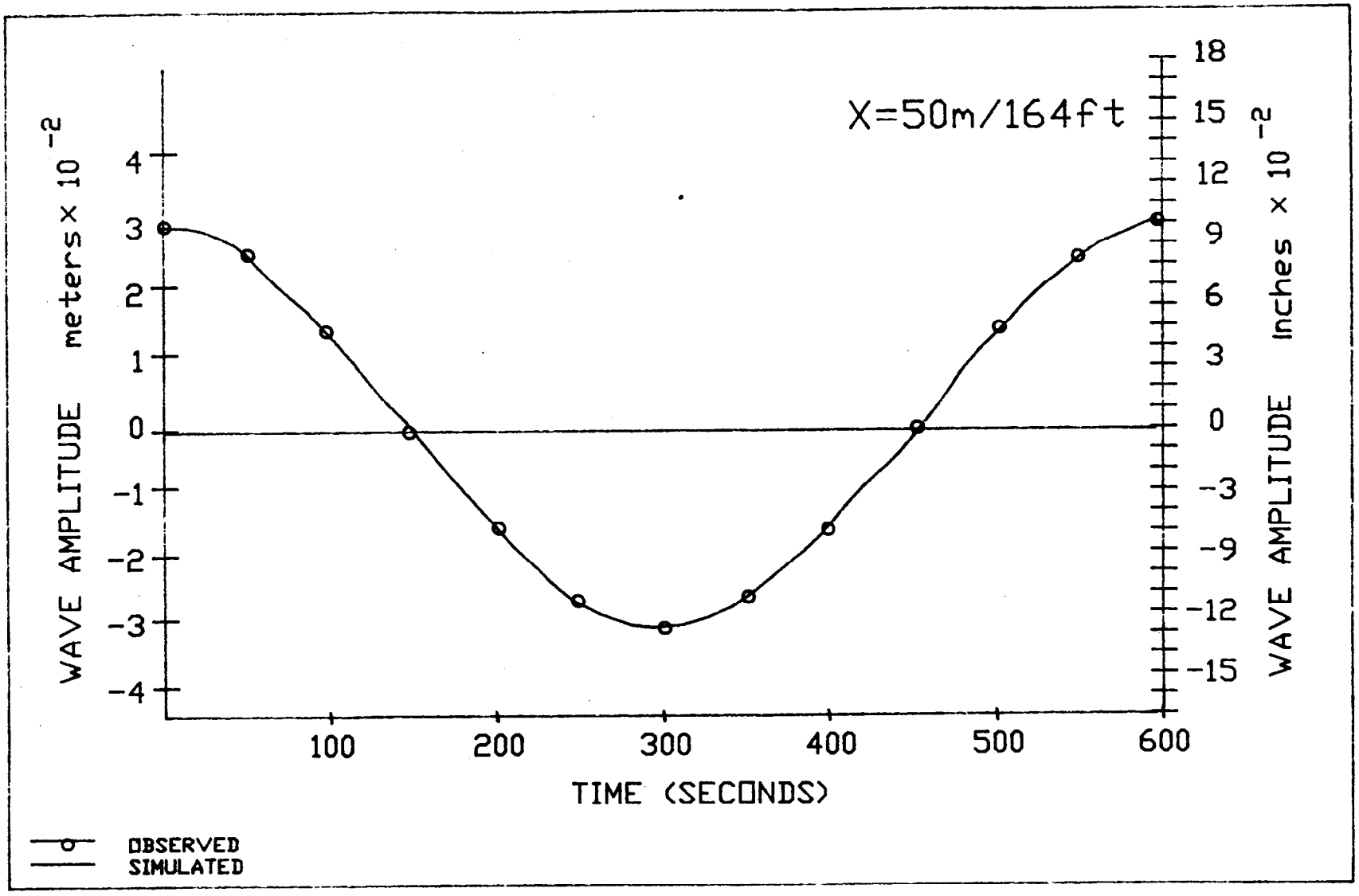

FIGURE 12 Comparison Between Observed and Simulated Experimental Tidal Data

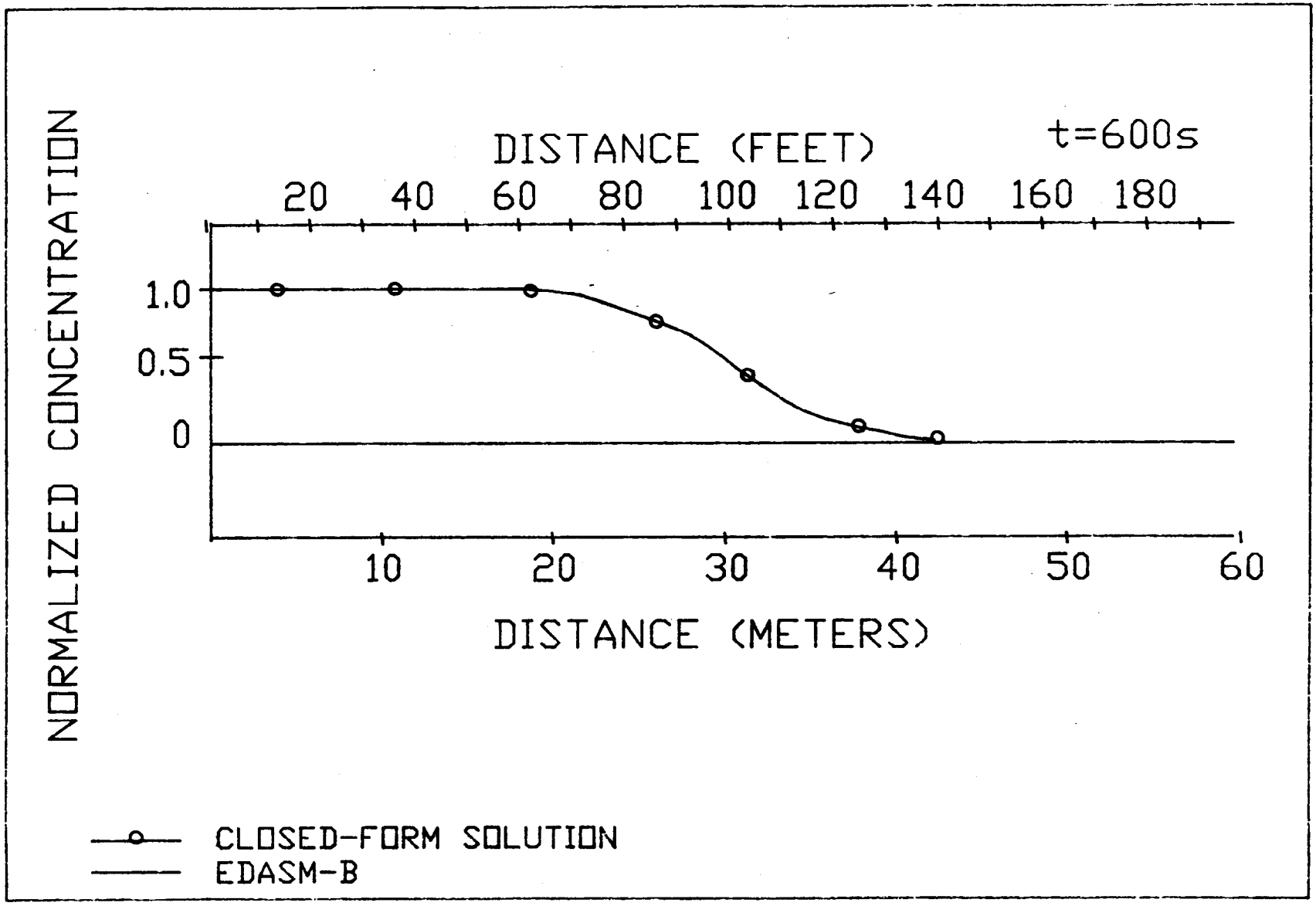

FIGURE 13 Comparison Between Closed-form and Numerical Solution for Salinity Distribution

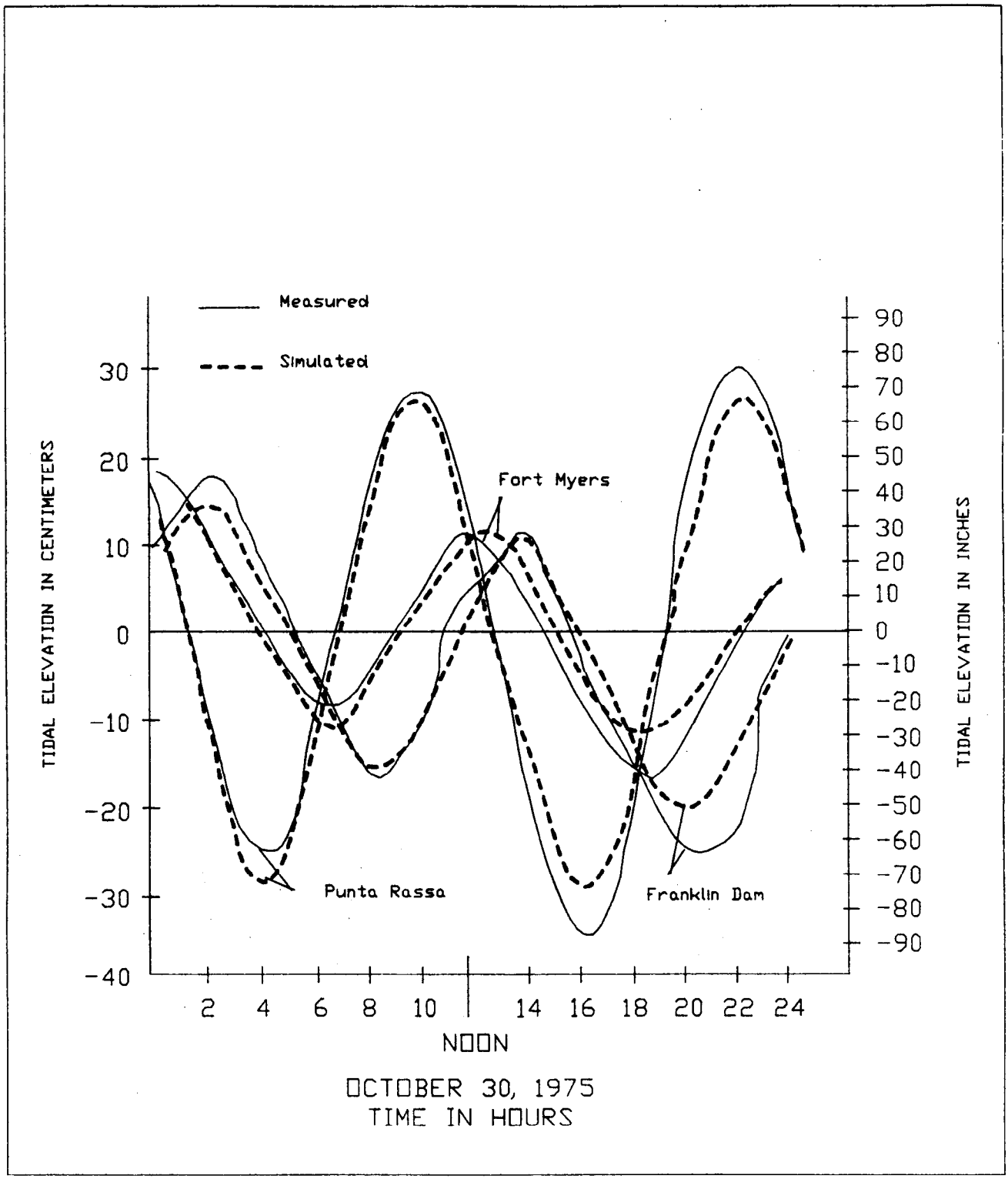

FIGURE 14 Simulated and Observed Hydrodynamic Data at Caloosahatchee Estuary

In general, the EDASM-B model seems to adequately simulate the hydrodynamics and longitudinal salinity distribution of one-dimensional estuarine systems.

SUMMARY, CONCLUSIONS AND SUGGESTIONS

A one-dimensional numerical model (EDASM-B) has been developed for the simulation of the hydrodynamics and salinity distribution of the Caloosahatchee River estuarine system. The model is based on the full dynamic St. Venant system of equations for the hydrodynamic part, and on the advection-dispersion equation for the salinity distribution part. The St. Venant system is solved by the leap-frog explicit numerical scheme, while the advection dispersion equation by the Crank-Nicholson implicit scheme. Model results showed agreement with laboratory data and closed-form solutions. Limited testing showed the potential of the model as a management tool for the Caloosahatchee estuary.

Synoptic field data, at least for a full tidal period (25 hrs), are necessary for a detailed calibration and verification of the estuarine system. Those data must be taken at the two estuarine boundaries, and at two arbitrary internal points (one for calibration and one for verification). Plans for data collection are made for FY 1988-89.

Improving the efficiency of the model can be achieved by writing the program in FORTRAN and using a FORTRAN compiler so that the program still operates on the PC level. This will substantially decrease the running time of the model.

LITERATURE CITED

Ames, W. F., 1977. Numerical methods for partial differential equations. 2nd edition, Academic Press, New York.

Fan, A. and R. Burgess, 1983. Surface water availability of the Caloosahatchee basin. Technical Memorandum, Water Resources Division, Resource Planning Department, South Florida Water Management District, pp. 79.

Ippen, A. T., Ed., 1966. Estuary and coastline hydrodynamics. McGraw'Hill, New York.

Mahmood, K. and V. Yevjevich, Eds., 1975. Unsteady flow in open channels. Vol. I, II, Water Resources Publication, Fort Collins, Colorado.

McDowell, D. M. and B. A. O'Connor, 1977. Hydraulic behaviour of estuaries. MacMillan Press, London, Great Britain.

Reichard, R. P., 1985. Analysis of NOS tidal data: Fort Meyers region. A Report to the South Florida Water Management District, Dept. of Oceanography and Ocean Engineering, Florida Institute of Technology, Melbourne, Florida.

Prichard, D. W., 1967. Observations of circulation in coastal plain estuaries, in Estuaries (Ed. G. H. Lauff),. American Assoc. Adv. Sci., Publ. No. 83, Washington, D.C.

Scarlatos, P. D., 1981. A study of tidal disturbances in channels of finite length. Scientific Bulletin, Section 5, Volume H, Aristotelean University of Thessaloniki, Thessaloniki, Greece.

Scarlatos, P. D. and F. W. Morris, 1986. Data analysis for quantification of estuarine dynamics. Proceedings of the ASCE South Florida Section, Annual Meeting, West Palm Beach, September 19-20.

Schureman, P., 1958. Manual of harmonic analysis and prediciton tides. Special Report No. 98, CGS, US Department of Commerce, Washington, D.C.

Smith, D. B., 1955. A study of the hydrological conditions of the Caloosahatchee River basin. Report to the Central and Southern Florida Flood Control District, West Palm Beach, pp. 6-12.

APPENDIX A

CROSS SECTIONS OF THE CALOOSAHATCHEE ESTUARY

(Ref. Fig. 4)

APPENDIX A

CROSS SECTIONS OF THE CALOOSAHATCHEE ESTUARY

(Ref. Fig. 4)

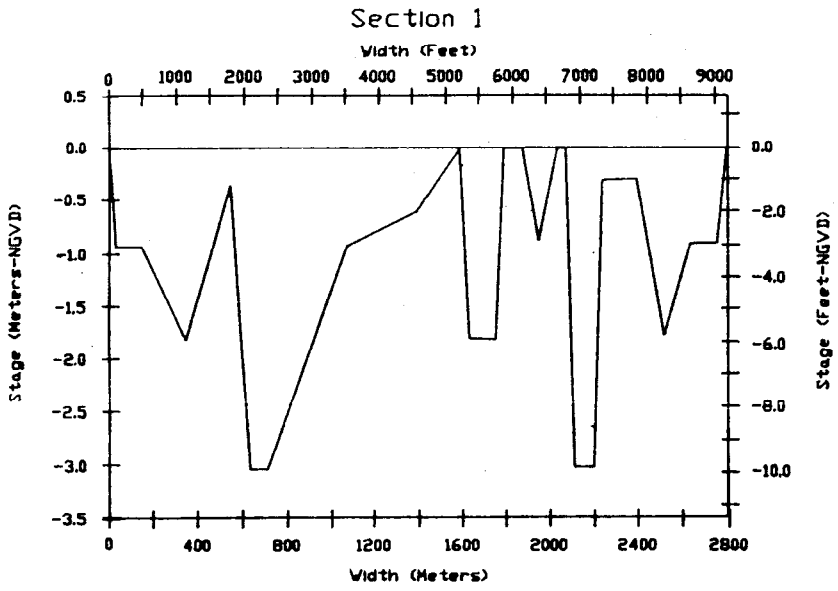
Section 1
Width (Feet)
0 1000 2000 3000 4000 5000 6000 7000 8000 9000
0.5 0.0 -0.5 -1.0 -1.5 -2.0 -2.5 -3.0 -3.5
0.0 -2.0 -4.0 -6.0 -8.0 -10.0
Stage (Meters-NGVD)
Stage (Feet-NGVD)
0 400 800 1200 1600 2000 2400 2800
Width (Meters)

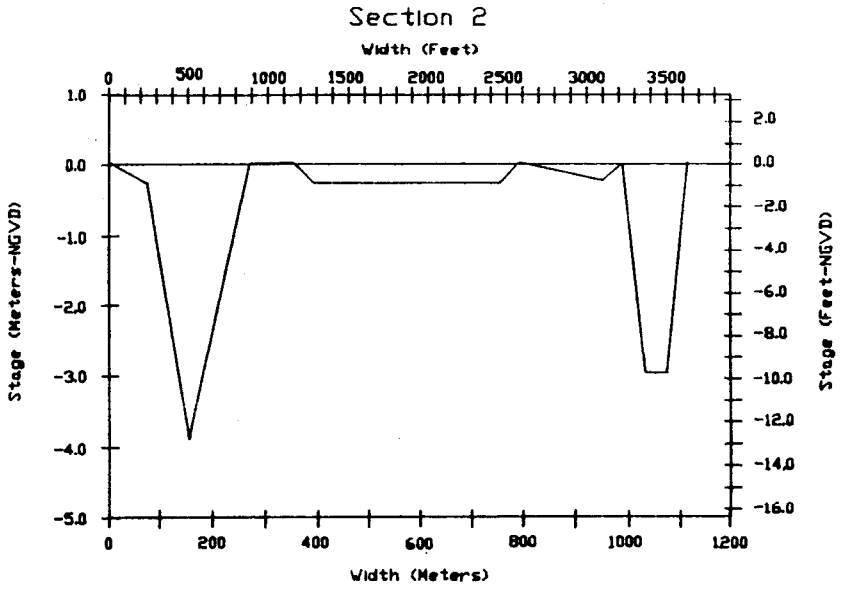
Section 2
Width (Feet)
0 500 1000 1500 2000 2500 3000 3500
1.0 0.0 -1.0 -2.0 -3.0 -4.0 -5.0
2.0 0.0 -2.0 -4.0 -6.0 -8.0 -10.0 -12.0 -14.0 -16.0
Stage (Meters-NGVD)
Stage (Feet-NGVD)
0 200 400 600 800 1000 1200
Width (Meters)

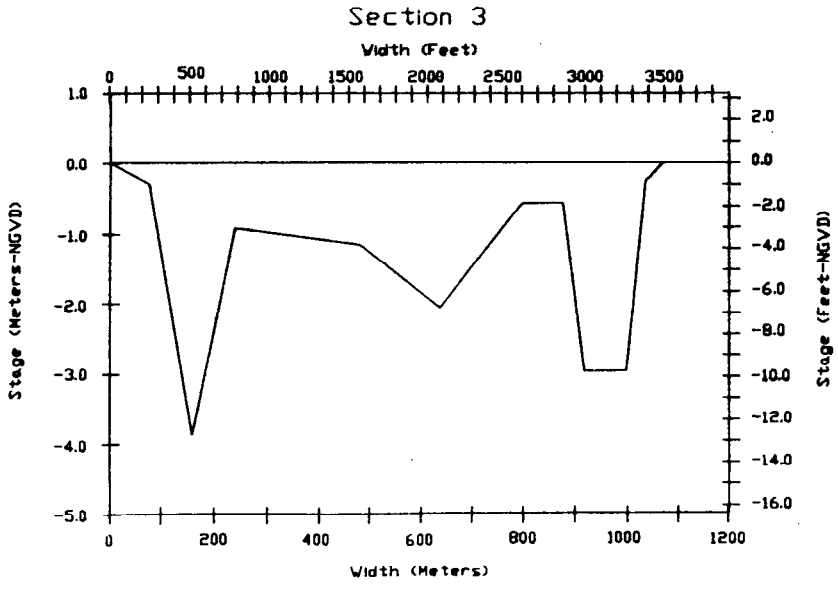
Section 3
Width (Feet)
0 500 1000 1500 2000 2500 3000 3500
1.0 0.0 -1.0 -2.0 -3.0 -4.0 -5.0
2.0 0.0 -2.0 -4.0 -6.0 -8.0 -10.0 -12.0 -14.0 -16.0
Stage (Meters-NGVD)
Stage (Feet-NGVD)
0 200 400 600 800 1000 1200
Width (Meters)

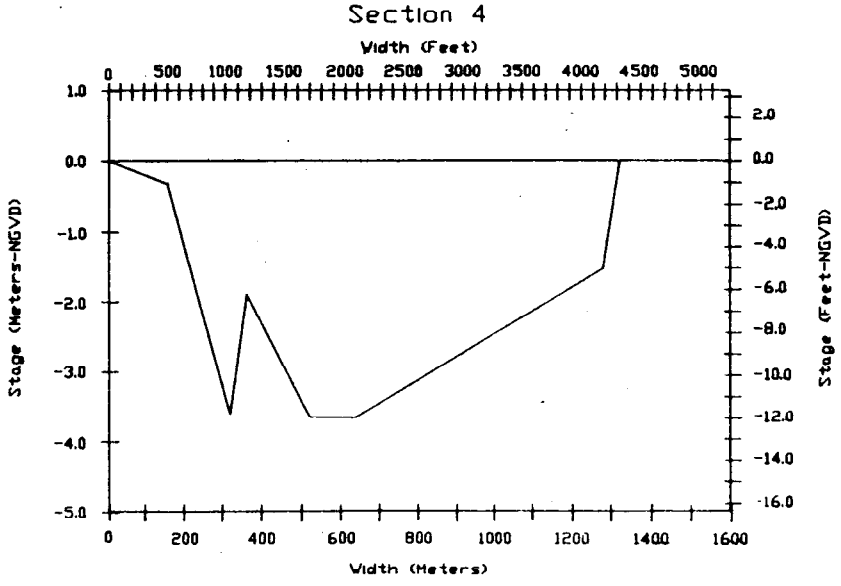
Section 4
Width (Feet)
0 500 1000 1500 2000 2500 3000 3500 4000 4500 5000
1.0 0.0 -1.0 -2.0 -3.0 -4.0 -5.0
2.0 0.0 -2.0 -4.0 -6.0 -8.0 -10.0 -12.0 -14.0 -16.0
Stage (Meters-NGVD)
Stage (Feet-NGVD)
0 200 400 600 800 1000 1200 1400 1600
Width (Meters)

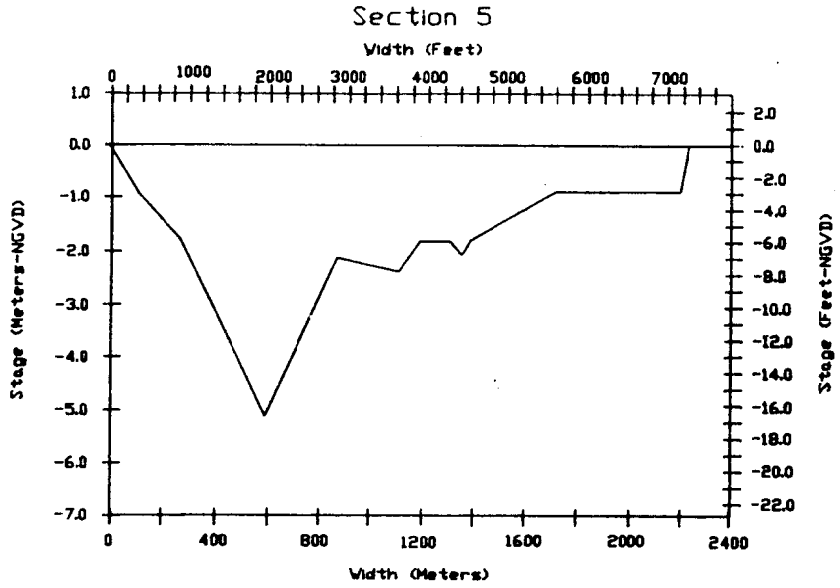
Section 5
Width (Feet)
0 1000 2000 3000 4000 5000 6000 7000
1.0 0.0 -1.0 -2.0 -3.0 -4.0 -5.0 -6.0 -7.0
2.0 0.0 -2.0 -4.0 -6.0 -8.0 -10.0 -12.0 -14.0 -16.0 -18.0 -20.0 -22.0
Stage (Meters-NGVD)
Stage (Feet-NGVD)
0 400 800 1200 1600 2000 2400
Width (Meters)

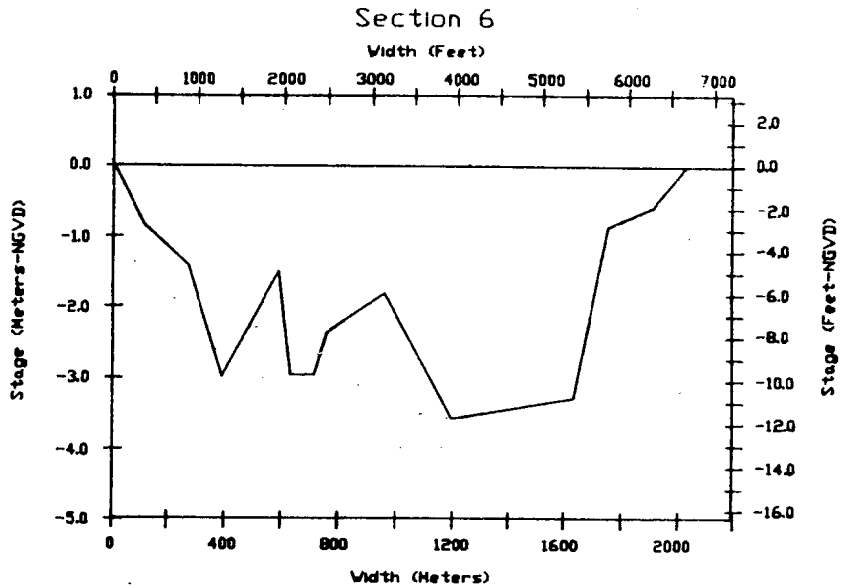
Section 6
Width (Feet)
0 1000 2000 3000 4000 5000 6000 7000
1.0 0.0 -1.0 -2.0 -3.0 -4.0 -5.0
2.0 0.0 -2.0 -4.0 -6.0 -8.0 -10.0 -12.0 -14.0 -16.0
Stage (Meters-NGVD)
Stage (Feet-NGVD)
0 400 800 1200 1600 2000
Width (Meters)

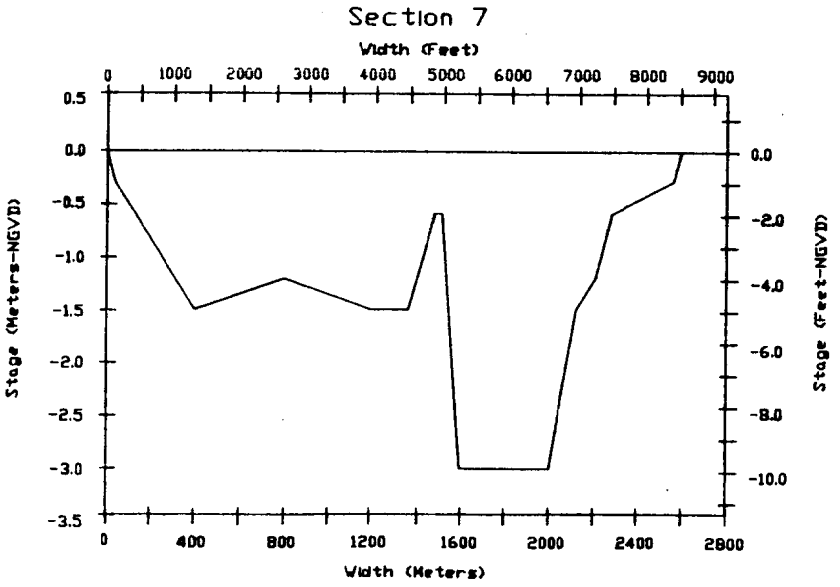
Section 7
Width (Feet)
0 1000 2000 3000 4000 5000 6000 7000 8000 9000
0.5 0.0 -0.5 -1.0 -1.5 -2.0 -2.5 -3.0 -3.5
0.0 -2.0 -4.0 -6.0 -8.0 -10.0
Stage (Meters-NGVD)
Stage (Feet-NGVD)
0 400 800 1200 1600 2000 2400 2800
Width (Meters)

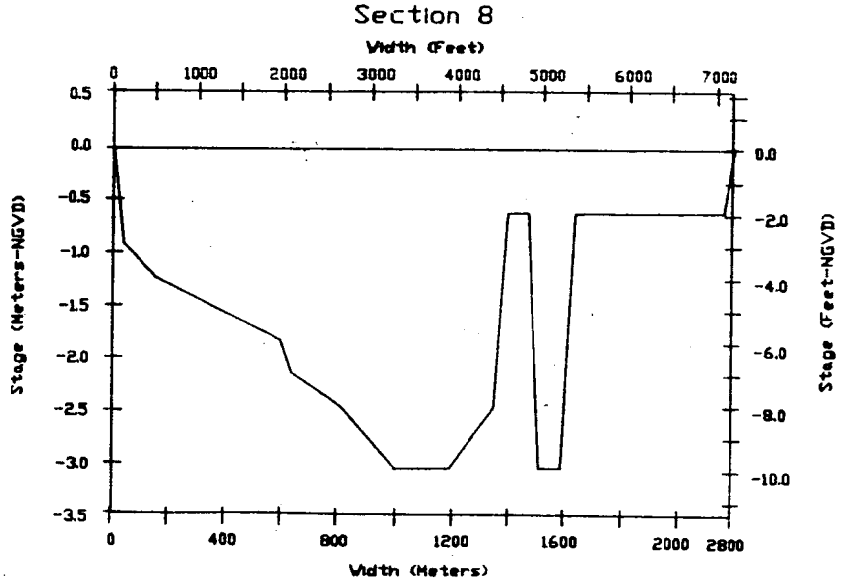
Section 8
Width (Feet)
0 1000 2000 3000 4000 5000 6000 7000
0.5 0.0 -0.5 -1.0 -1.5 -2.0 -2.5 -3.0 -3.5
0.0 -2.0 -4.0 -6.0 -8.0 -10.0
Stage (Meters-NGVD)
Stage (Feet-NGVD)
0 400 800 1200 1600 2000 2800
Width (Meters)

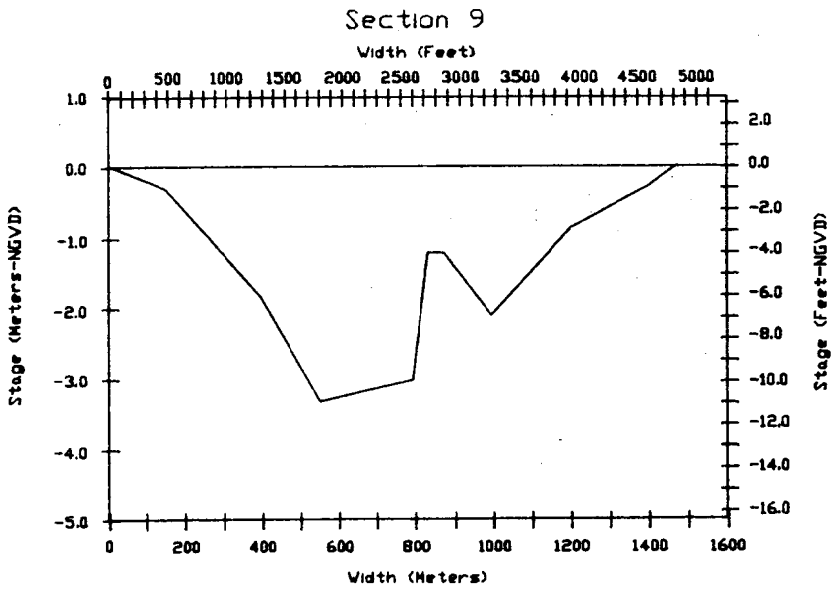
Section 9
Width (Feet)
0 500 1000 1500 2000 2500 3000 3500 4000 4500 5000
Stage (Meters-NGVD)
1.0 0.0 -1.0 -2.0 -3.0 -4.0 -5.0
Stage (Feet-NGVD)
2.0 0.0 -2.0 -4.0 -6.0 -8.0 -10.0 -12.0 -14.0 -16.0
0 200 400 600 800 1000 1200 1400 1600
Width (Meters)

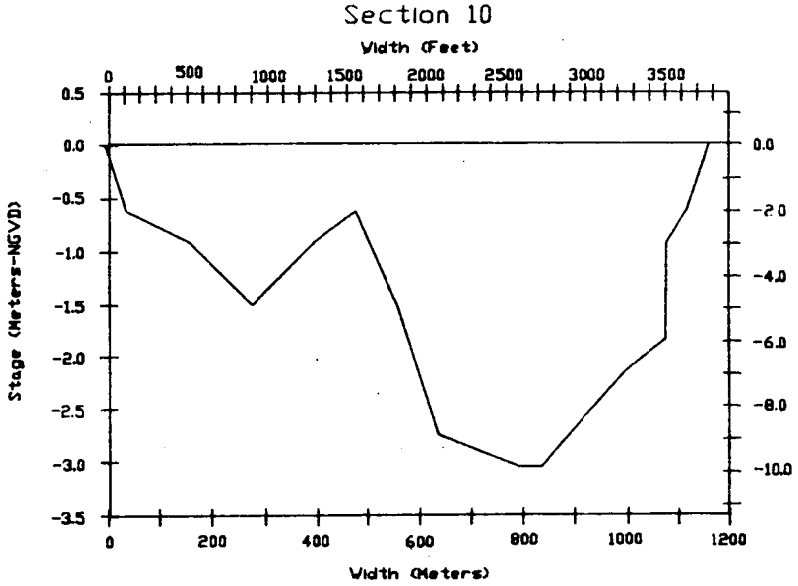
Section 10
Width (Feet)
0 500 1000 1500 2000 2500 3000 3500
Stage (Meters-NGVD)
0.5 0.0 -0.5 -1.0 -1.5 -2.0 -2.5 -3.0 -3.5
Stage (Feet-NGVD)
0.0 -2.0 -4.0 -6.0 -8.0 -10.0
0 200 400 600 800 1000 1200
Width (Meters)

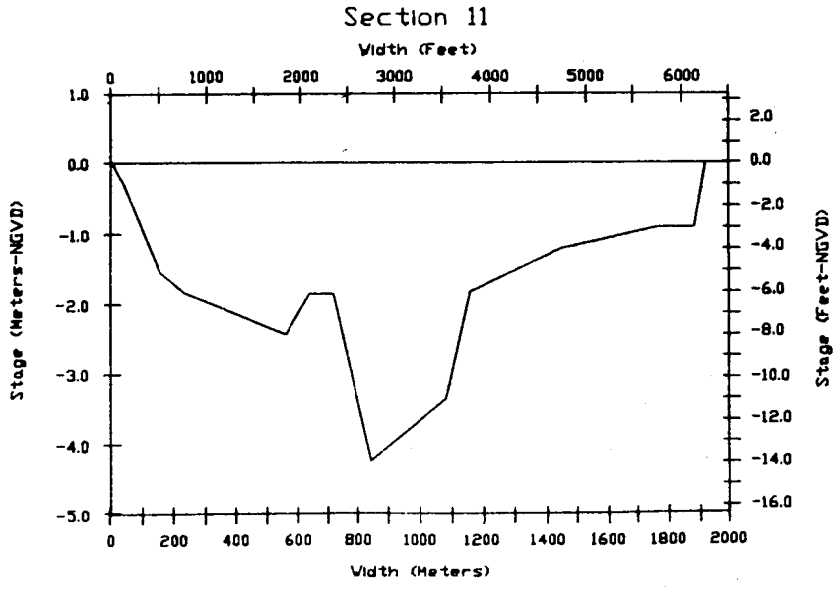
Section 11
Width (Feet)
0 1000 2000 3000 4000 5000 6000
Stage (Meters-NGVD)
1.0 0.0 -1.0 -2.0 -3.0 -4.0 -5.0
Stage (Feet-NGVD)
2.0 0.0 -2.0 -4.0 -6.0 -8.0 -10.0 -12.0 -14.0 -16.0
0 200 400 600 800 1000 1200 1400 1600 1800 2000
Width (Meters)

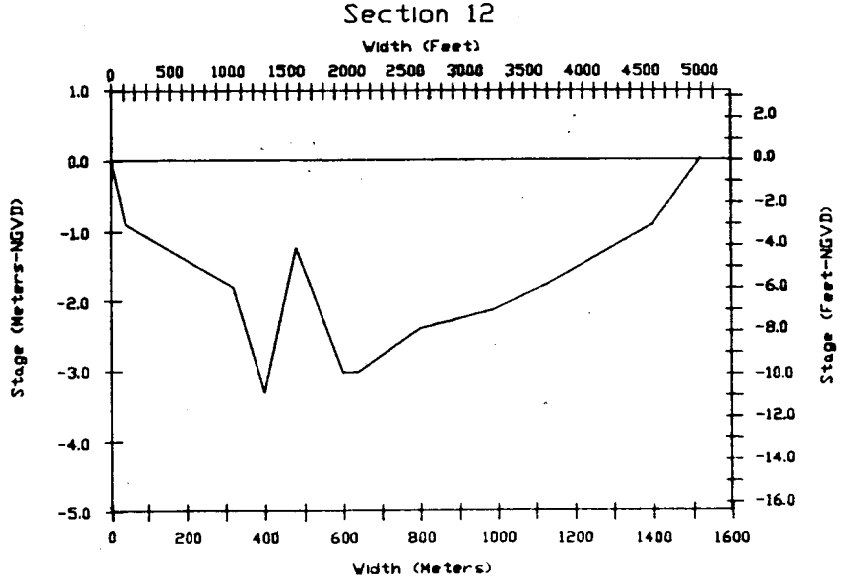
Section 12
Width (Feet)
0 500 1000 1500 2000 2500 3000 3500 4000 4500 5000
Stage (Meters-NGVD)
1.0 0.0 -1.0 -2.0 -3.0 -4.0 -5.0
Stage (Feet-NGVD)
2.0 0.0 -2.0 -4.0 -6.0 -8.0 -10.0 -12.0 -14.0 -16.0
0 200 400 600 800 1000 1200 1400 1600
Width (Meters)

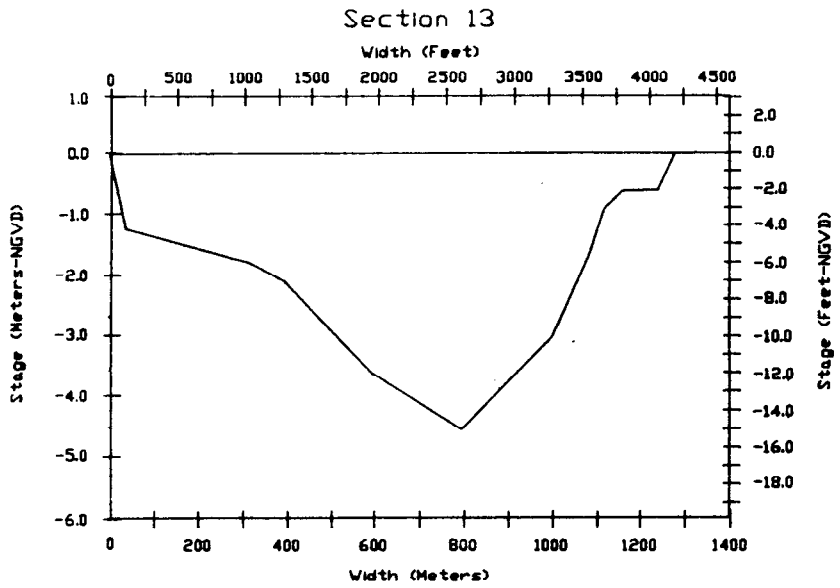
Section 13
Width (Feet)
0 500 1000 1500 2000 2500 3000 3500 4000 4500
Stage (Meters-NGVD)
1.0 0.0 -1.0 -2.0 -3.0 -4.0 -5.0 -6.0
Stage (Feet-NGVD)
2.0 0.0 -2.0 -4.0 -6.0 -8.0 -10.0 -12.0 -14.0 -16.0 -18.0
0 200 400 600 800 1000 1200 1400
Width (Meters)

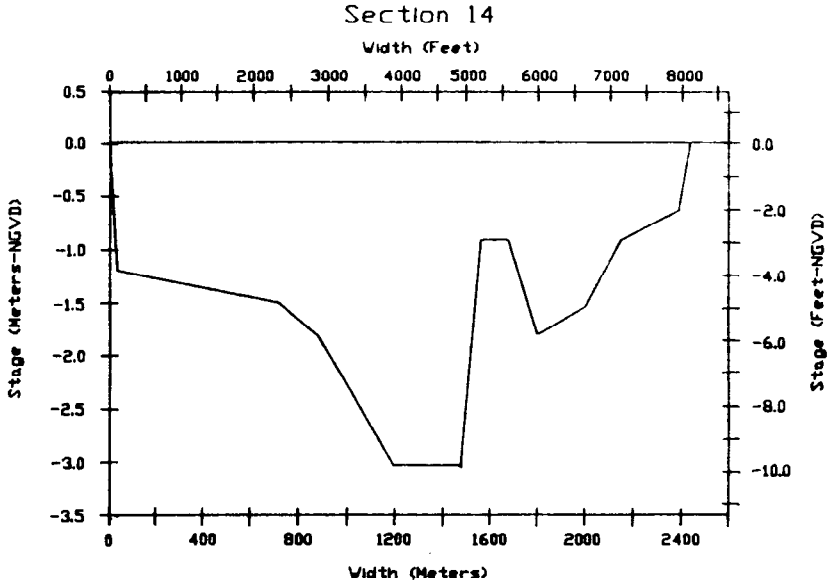
Section 14
Width (Feet)
0 1000 2000 3000 4000 5000 6000 7000 8000
Stage (Meters-NGVD)
0.5 0.0 -0.5 -1.0 -1.5 -2.0 -2.5 -3.0 -3.5
Stage (Feet-NGVD)
0.0 -2.0 -4.0 -6.0 -8.0 -10.0
0 400 800 1200 1600 2000 2400
Width (Meters)

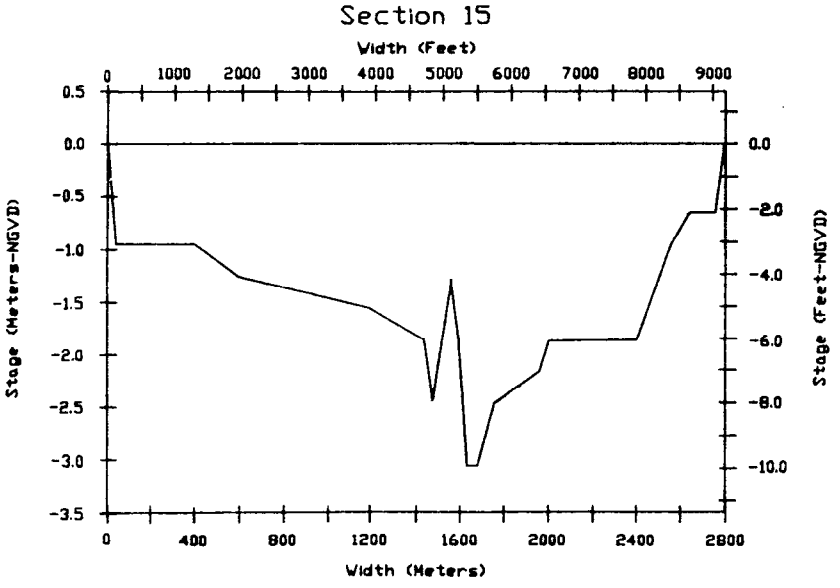
Section 15
Width (Feet)
0 1000 2000 3000 4000 5000 6000 7000 8000 9000
Stage (Meters-NGVD)
0.5 0.0 -0.5 -1.0 -1.5 -2.0 -2.5 -3.0 -3.5
Stage (Feet-NGVD)
0.0 -2.0 -4.0 -6.0 -8.0 -10.0
0 400 800 1200 1600 2000 2400 2800
Width (Meters)

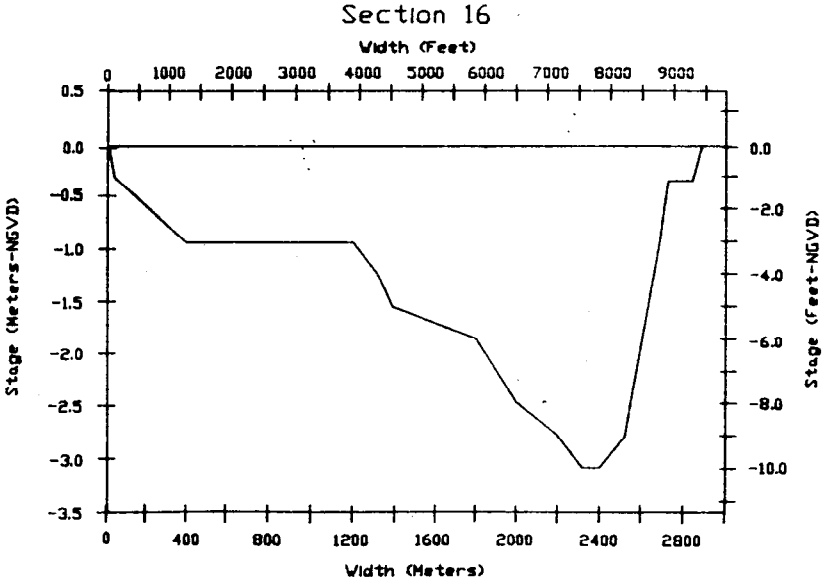
Section 16
Width (Feet)
0 1000 2000 3000 4000 5000 6000 7000 8000 9000
Stage (Meters-NGVD)
0.5 0.0 -0.5 -1.0 -1.5 -2.0 -2.5 -3.0 -3.5
Stage (Feet-NGVD)
0.0 -2.0 -4.0 -6.0 -8.0 -10.0
0 400 800 1200 1600 2000 2400 2800
Width (Meters)

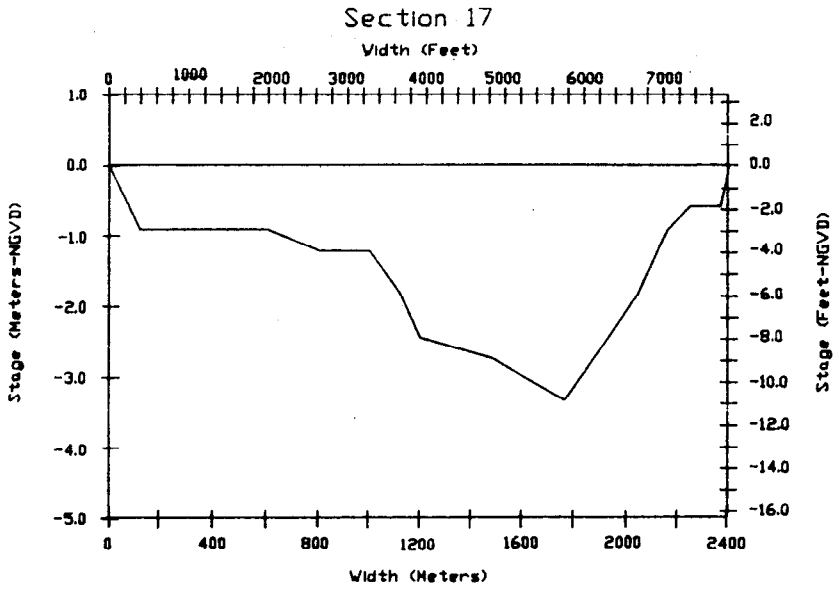
Section 17
Width (Feet)
0 1000 2000 3000 4000 5000 6000 7000
1.0 0.0 -1.0 -2.0 -3.0 -4.0 -5.0
2.0 0.0 -2.0 -4.0 -6.0 -8.0 -10.0 -12.0 -14.0 -16.0
Stage (Meters-NGVD)
Stage (Feet-NGVD)
0 400 800 1200 1600 2000 2400
Width (Meters)

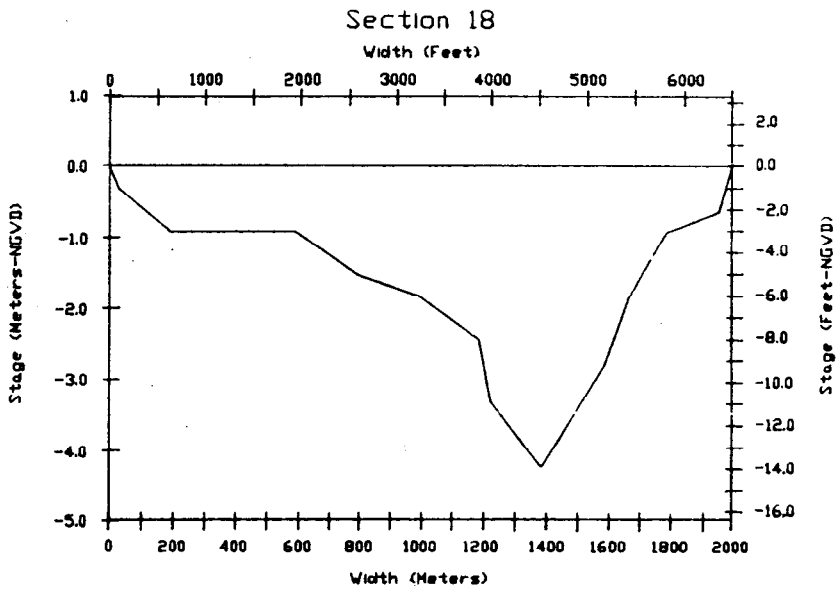
Section 18
Width (Feet)
0 1000 2000 3000 4000 5000 6000
1.0 0.0 -1.0 -2.0 -3.0 -4.0 -5.0
2.0 0.0 -2.0 -4.0 -6.0 -8.0 -10.0 -12.0 -14.0 -16.0
Stage (Meters-NGVD)
Stage (Feet-NGVD)
0 200 400 600 800 1000 1200 1400 1600 1800 2000
Width (Meters)

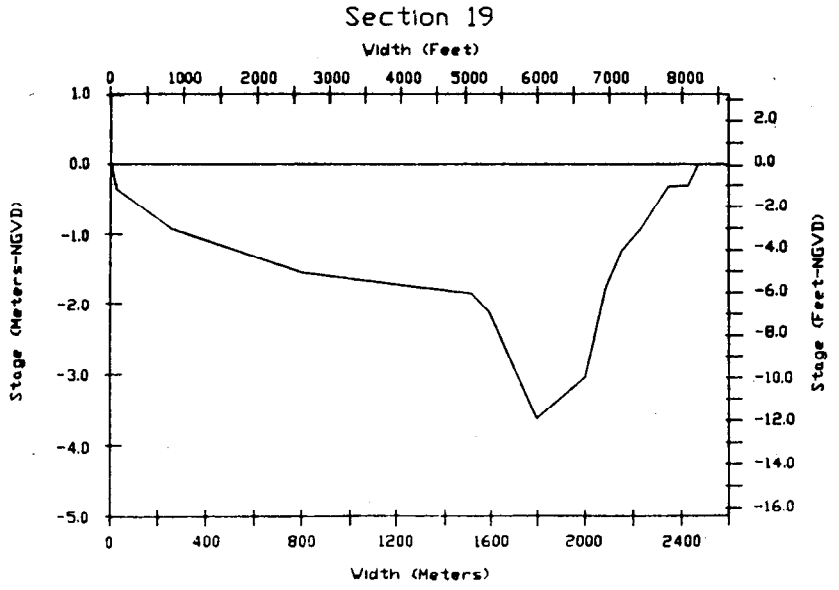
Section 19
Width (Feet)
0 1000 2000 3000 4000 5000 6000 7000 8000
1.0 0.0 -1.0 -2.0 -3.0 -4.0 -5.0
2.0 0.0 -2.0 -4.0 -6.0 -8.0 -10.0 -12.0 -14.0 -16.0
Stage (Meters-NGVD)
Stage (Feet-NGVD)
0 400 800 1200 1600 2000 2400
Width (Meters)

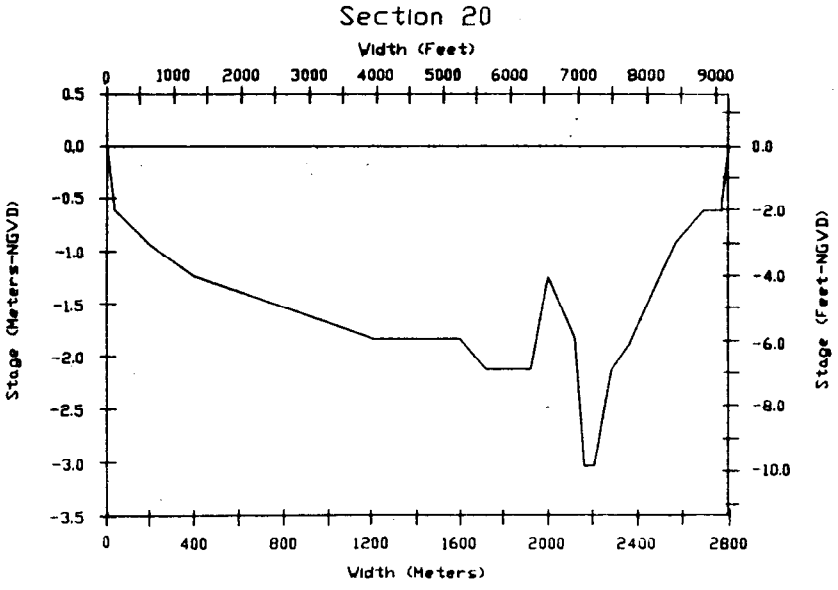
Section 20
Width (Feet)
0 1000 2000 3000 4000 5000 6000 7000 8000 9000
0.5 0.0 -0.5 -1.0 -1.5 -2.0 -2.5 -3.0 -3.5
0.0 -2.0 -4.0 -6.0 -8.0 -10.0
Stage (Meters-NGVD)
Stage (Feet-NGVD)
0 400 800 1200 1600 2000 2400 2800
Width (Meters)

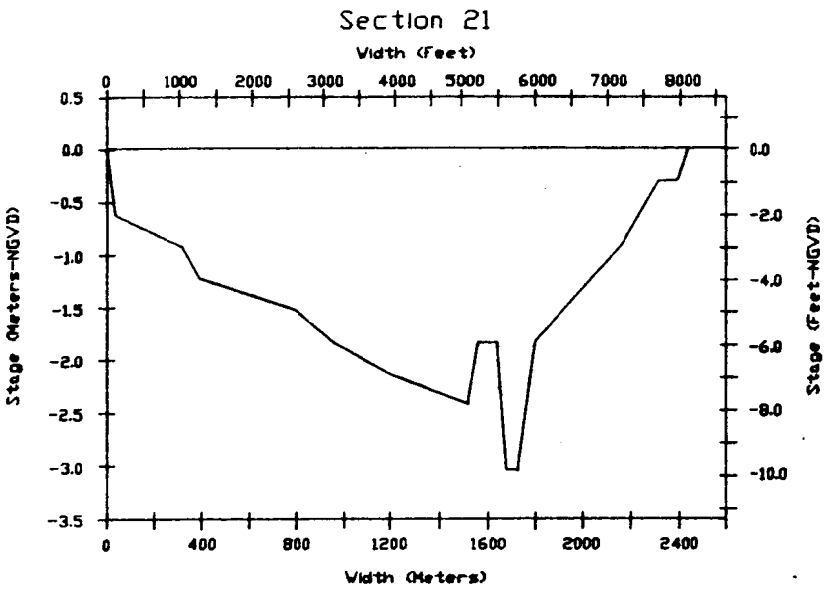
Section 21
Width (Feet)
0 1000 2000 3000 4000 5000 6000 7000 8000
0.5 0.0 -0.5 -1.0 -1.5 -2.0 -2.5 -3.0 -3.5
0.0 -2.0 -4.0 -6.0 -8.0 -10.0
Stage (Meters-NGVD)
Stage (Feet-NGVD)
0 400 800 1200 1600 2000 2400
Width (Meters)

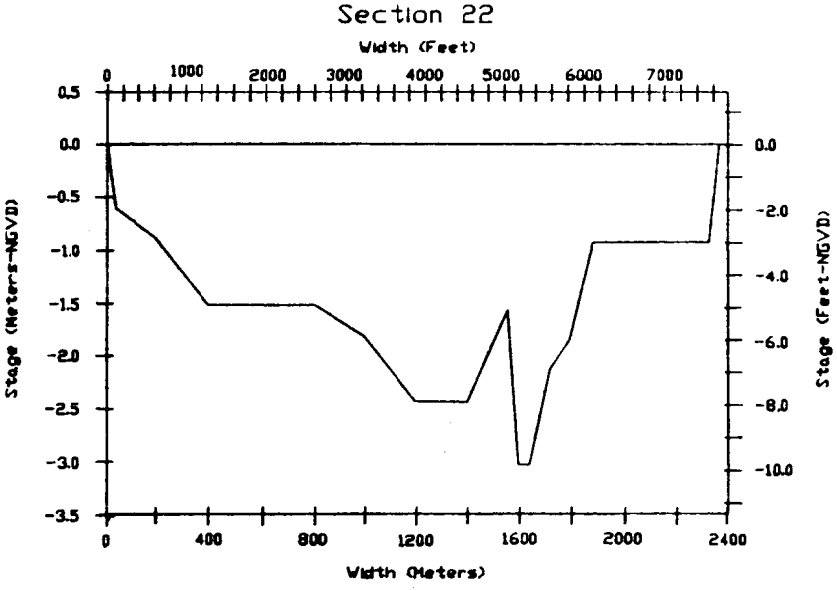
Section 22
Width (Feet)
0 1000 2000 3000 4000 5000 6000 7000
0.5 0.0 -0.5 -1.0 -1.5 -2.0 -2.5 -3.0 -3.5
0.0 -2.0 -4.0 -6.0 -8.0 -10.0
Stage (Meters-NGVD)
Stage (Feet-NGVD)
0 400 800 1200 1600 2000 2400
Width (Meters)

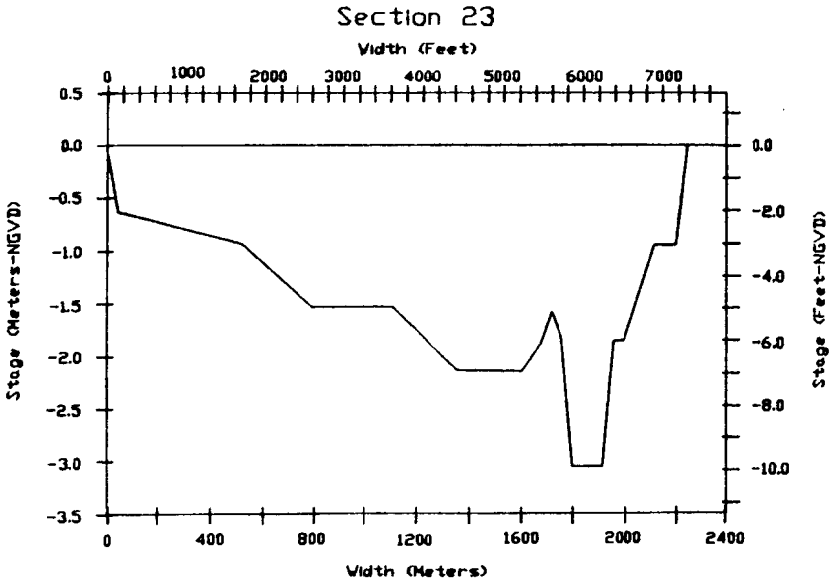
Section 23
Width (Feet)
0 1000 2000 3000 4000 5000 6000 7000
0.5 0.0 -0.5 -1.0 -1.5 -2.0 -2.5 -3.0 -3.5
0.0 -2.0 -4.0 -6.0 -8.0 -10.0
Stage (Meters-NGVD)
Stage (Feet-NGVD)
0 400 800 1200 1600 2000 2400
Width (Meters)

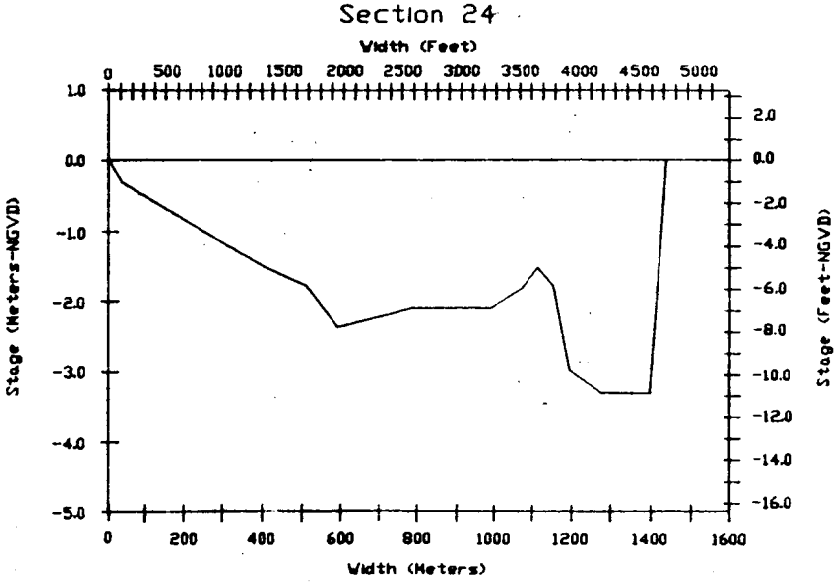
Section 24
Width (Feet)
0 500 1000 1500 2000 2500 3000 3500 4000 4500 5000
1.0 0.0 -1.0 -2.0 -3.0 -4.0 -5.0
2.0 0.0 -2.0 -4.0 -6.0 -8.0 -10.0 -12.0 -14.0 -16.0
Stage (Meters-NGVD)
Stage (Feet-NGVD)
0 200 400 600 800 1000 1200 1400 1600
Width (Meters)

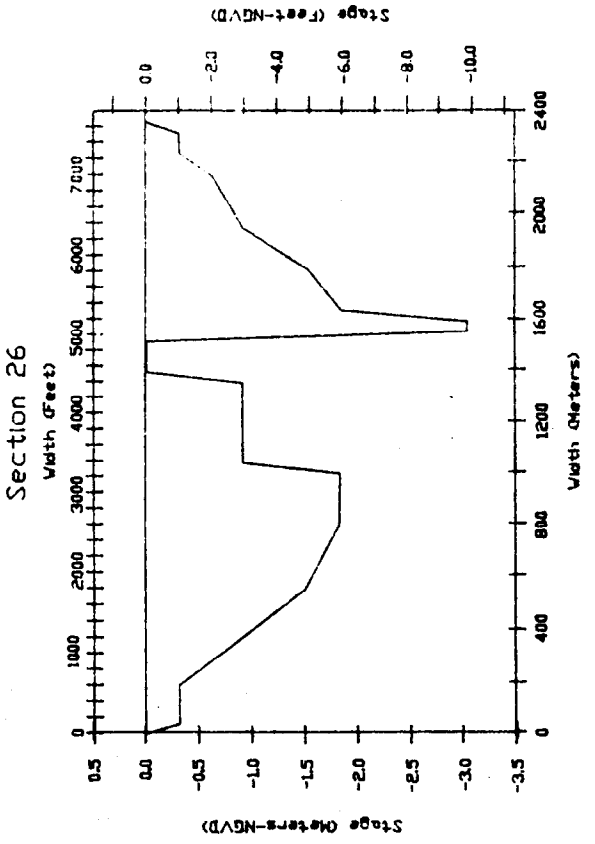
Section 26
Width (Feet)
Width (Meters)
Stage (Feet-NGVD)
Stage (Meters-NGVD)

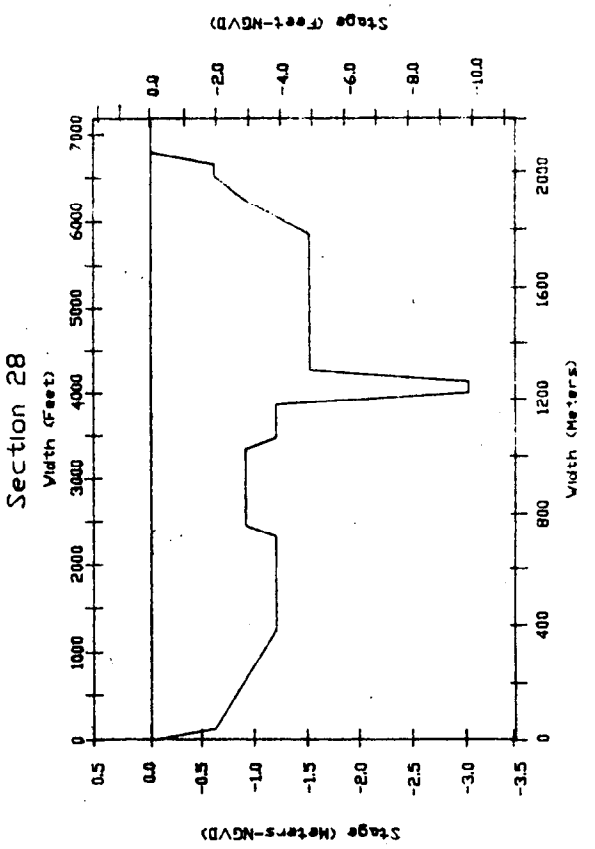
Section 28
Width (Feet)
Width (Meters)
Stage (Feet-NGVD)
Stage (Meters-NGVD)

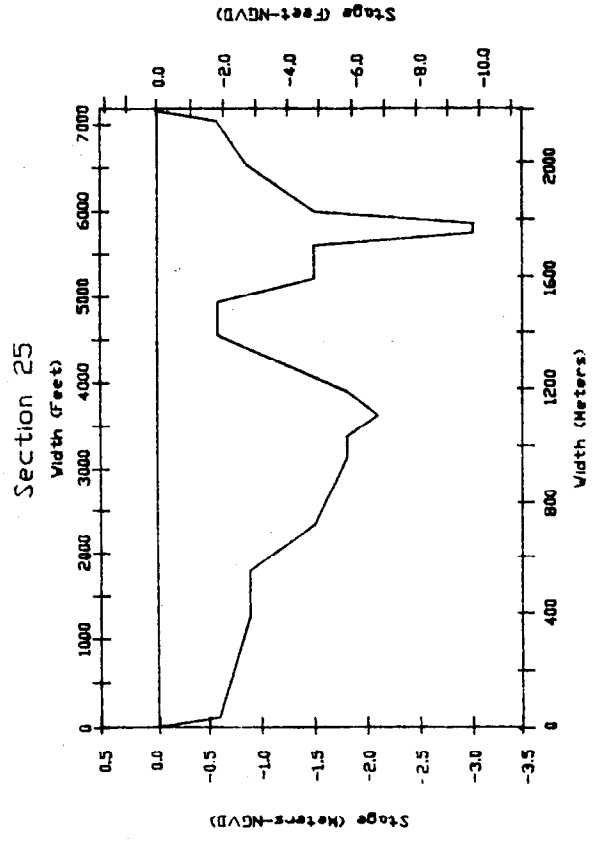
Section 25
Width (Feet)
Width (Meters)
Stage (Feet-NGVD)
Stage (Meters-NGVD)

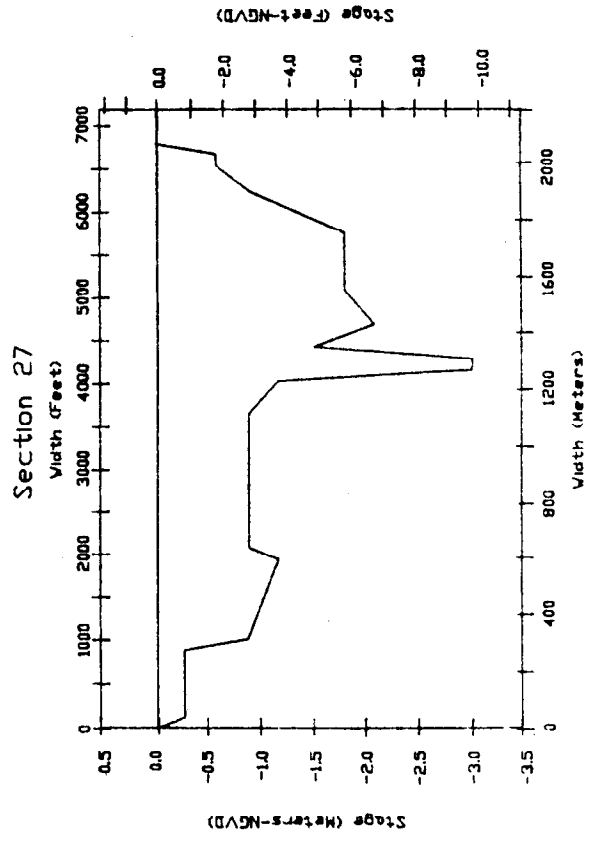
Section 27
Width (Feet)
Width (Meters)
Stage (Feet-NGVD)
Stage (Meters-NGVD)

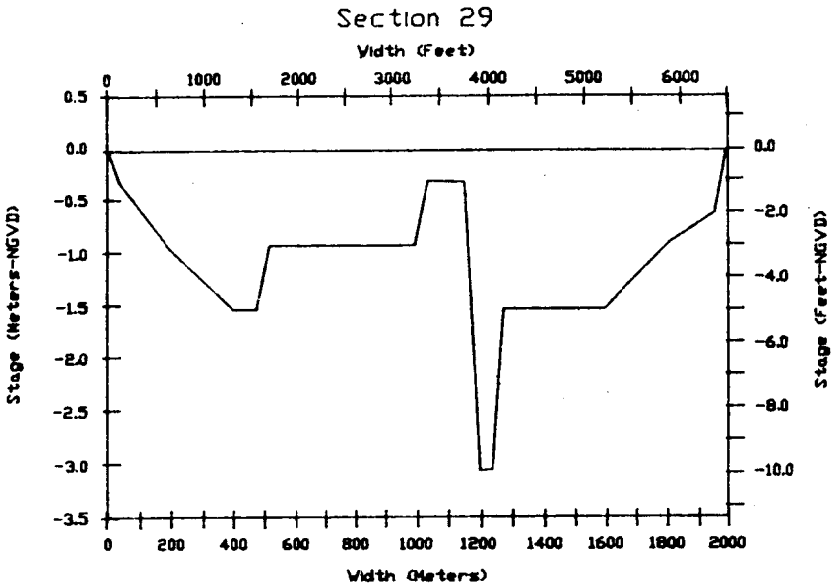
Section 29
Width (Feet)
0 1000 2000 3000 4000 5000 6000
0.5 0.0 -0.5 -1.0 -1.5 -2.0 -2.5 -3.0 -3.5
Stage (Meters-NGVD)
0.0 -2.0 -4.0 -6.0 -8.0 -10.0
Stage (Feet-NGVD)
0 200 400 600 800 1000 1200 1400 1600 1800 2000
Width (Meters)

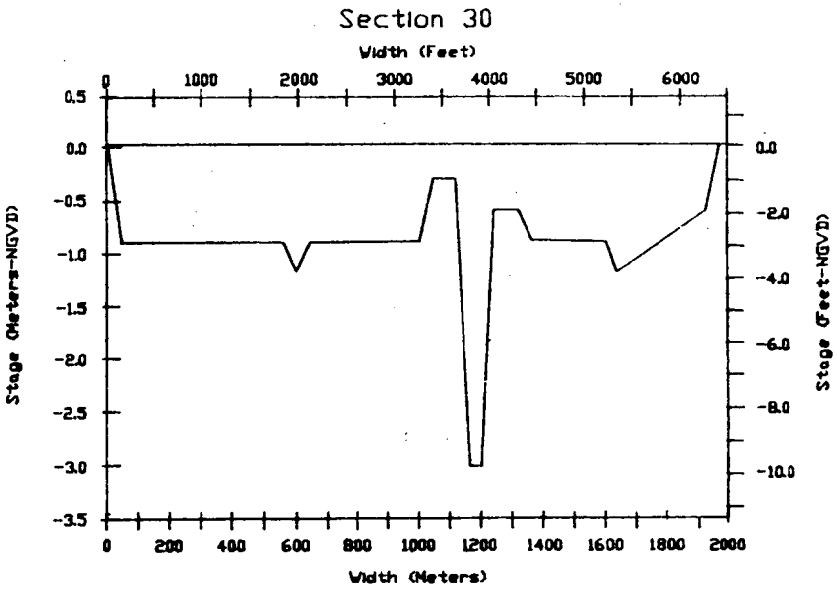
Section 30
Width (Feet)
0 1000 2000 3000 4000 5000 6000
0.5 0.0 -0.5 -1.0 -1.5 -2.0 -2.5 -3.0 -3.5
Stage (Meters-NGVD)
0.0 -2.0 -4.0 -6.0 -8.0 -10.0
Stage (Feet-NGVD)
0 200 400 600 800 1000 1200 1400 1600 1800 2000
Width (Meters)

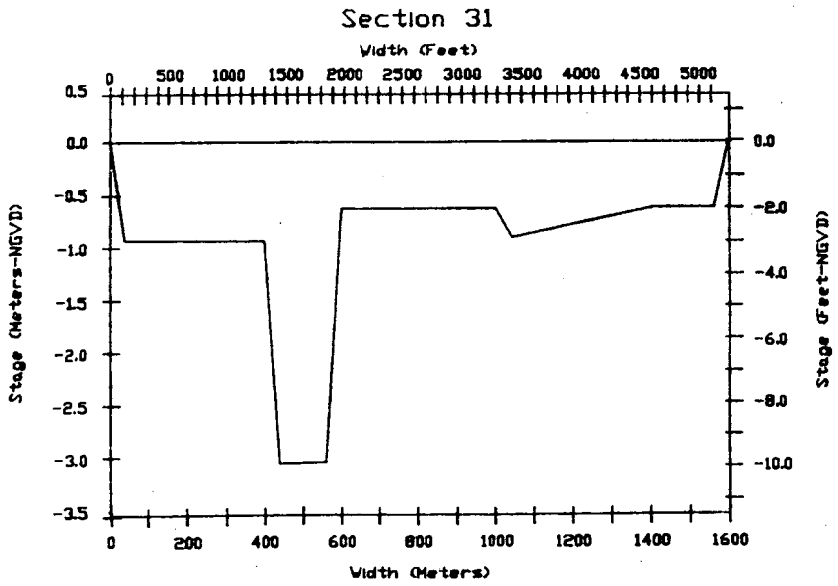
Section 31
Width (Feet)
0 500 1000 1500 2000 2500 3000 3500 4000 4500 5000
0.5 0.0 -0.5 -1.0 -1.5 -2.0 -2.5 -3.0 -3.5
Stage (Meters-NGVD)
0.0 -2.0 -4.0 -6.0 -8.0 -10.0
Stage (Feet-NGVD)
0 200 400 600 800 1000 1200 1400 1600
Width (Meters)

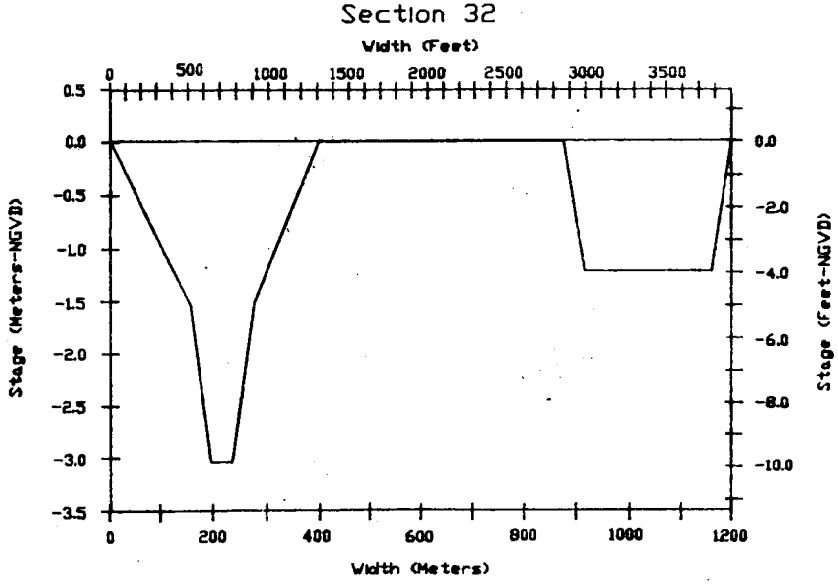
Section 32
Width (Feet)
0 500 1000 1500 2000 2500 3000 3500
0.5 0.0 -0.5 -1.0 -1.5 -2.0 -2.5 -3.0 -3.5
Stage (Meters-NGVD)
0.0 -2.0 -4.0 -6.0 -8.0 -10.0
Stage (Feet-NGVD)
0 200 400 600 800 1000 1200
Width (Meters)

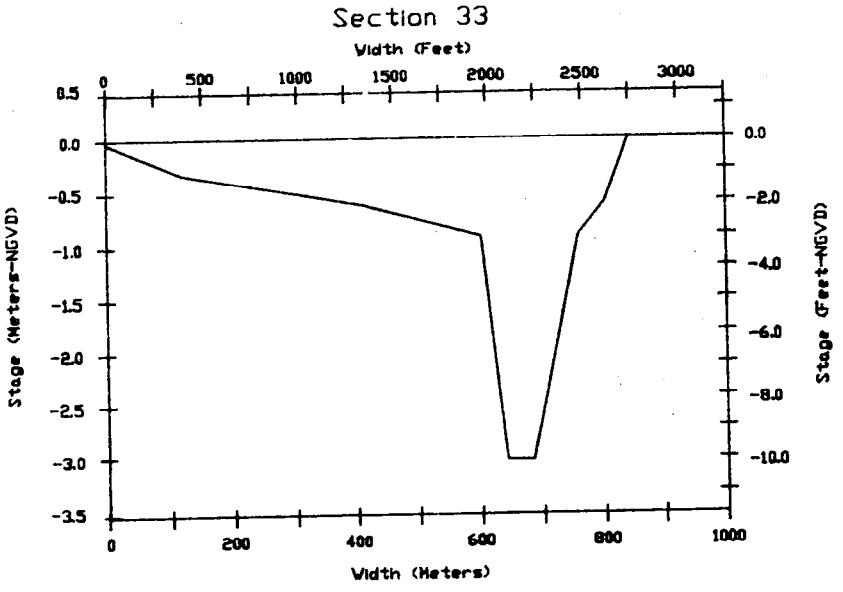
Section 33
Width (Feet)
0
500
1000
1500
2000
2500
3000
0.5
0.0
-0.5
-1.0
-1.5
-2.0
-2.5
-3.0
-3.5
Stage (Meters-NGVD)
0.0
-2.0
-4.0
-6.0
-8.0
-10.0
Stage (Feet-NGVD)
0
200
400
600
800
1000
Width (Meters)

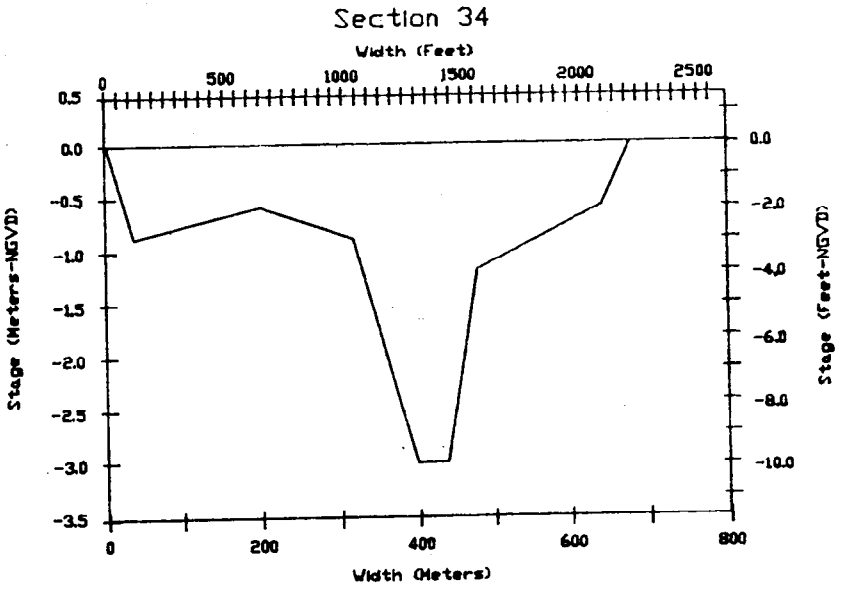
Section 34
Width (Feet)
0
500
1000
1500
2000
2500
0.5
0.0
-0.5
-1.0
-1.5
-2.0
-2.5
-3.0
-3.5
Stage (Meters-NGVD)
0.0
-2.0
-4.0
-6.0
-8.0
-10.0
Stage (Feet-NGVD)
0
200
400
600
800
Width (Meters)

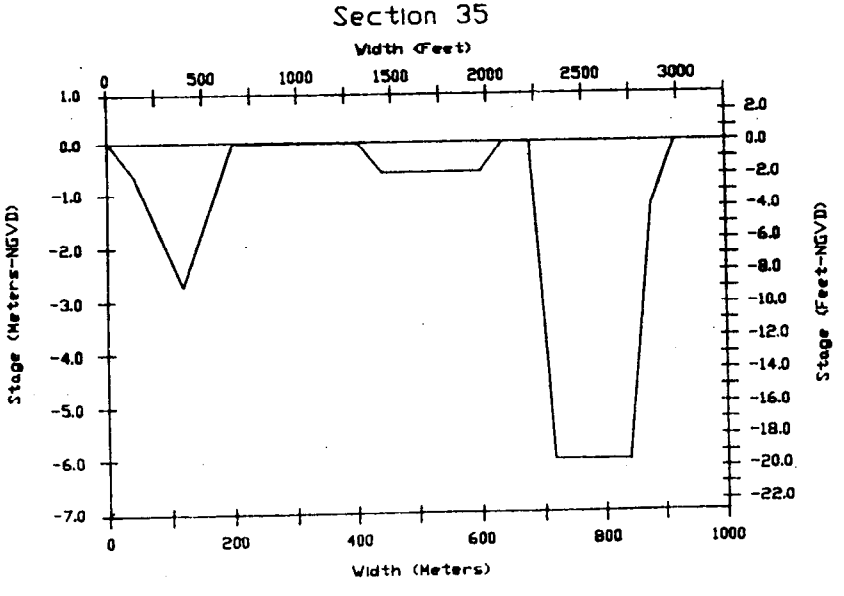
Section 35
Width (Feet)
0
500
1000
1500
2000
2500
3000
1.0
0.0
-1.0
-2.0
-3.0
-4.0
-5.0
-6.0
-7.0
Stage (Meters-NGVD)
2.0
0.0
-2.0
-4.0
-6.0
-8.0
-10.0
-12.0
-14.0
-16.0
-18.0
-20.0
-22.0
Stage (Feet-NGVD)
0
200
400
600
800
1000
Width (Meters)

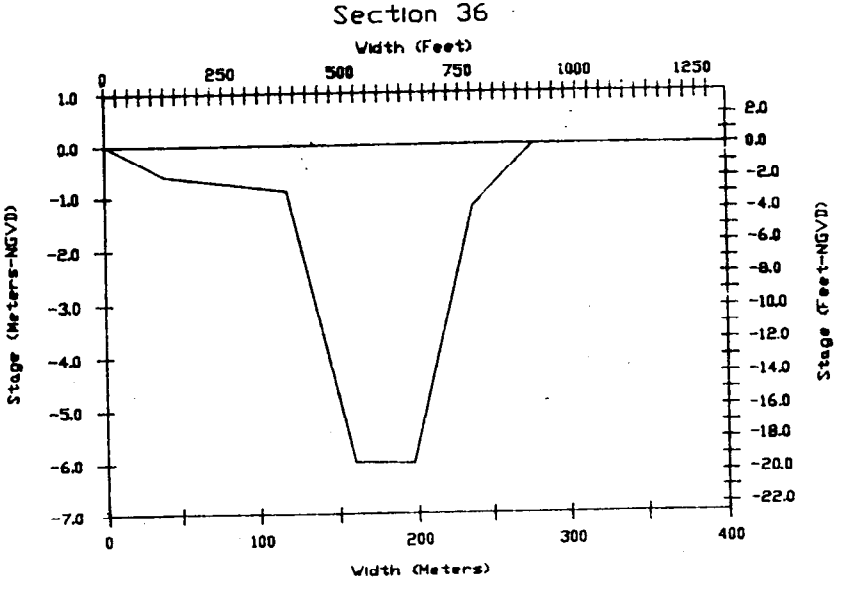
Section 36
Width (Feet)
0
250
500
750
1000
1250
1.0
0.0
-1.0
-2.0
-3.0
-4.0
-5.0
-6.0
-7.0
Stage (Meters-NGVD)
2.0
0.0
-2.0
-4.0
-6.0
-8.0
-10.0
-12.0
-14.0
-16.0
-18.0
-20.0
-22.0
Stage (Feet-NGVD)
0
100
200
300
400
Width (Meters)

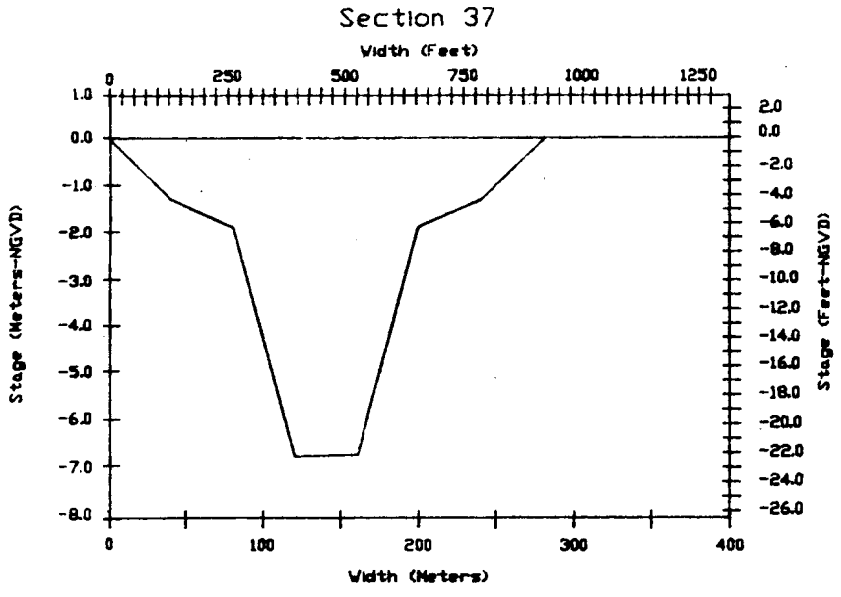
Section 37
Width (Feet)
0 250 500 750 1000 1250
Stage (Meters-NGVD)
1.0 0.0 -1.0 -2.0 -3.0 -4.0 -5.0 -6.0 -7.0 -8.0
Stage (Feet-NGVD)
2.0 0.0 -2.0 -4.0 -6.0 -8.0 -10.0 -12.0 -14.0 -16.0 -18.0 -20.0 -22.0 -24.0 -26.0
0 100 200 300 400
Width (Meters)

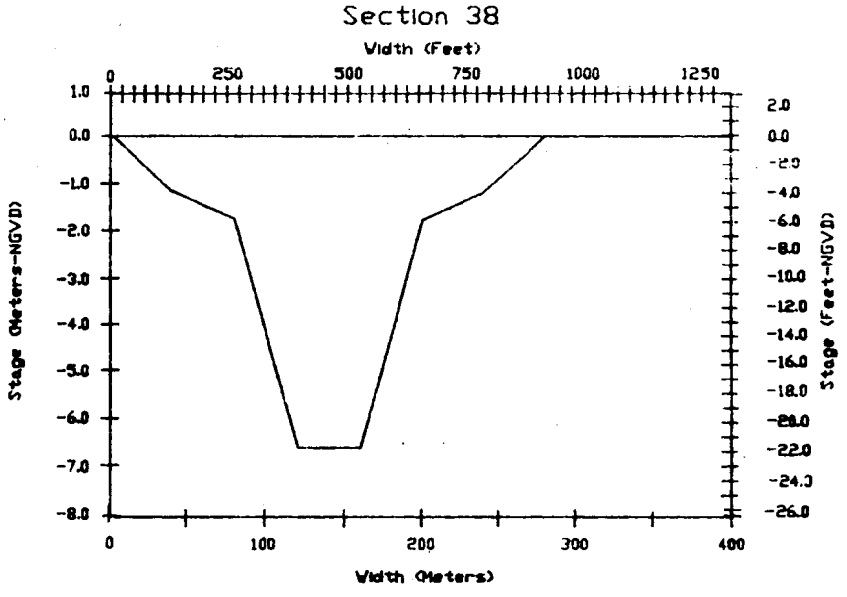
Section 38
Width (Feet)
0 250 500 750 1000 1250
Stage (Meters-NGVD)
1.0 0.0 -1.0 -2.0 -3.0 -4.0 -5.0 -6.0 -7.0 -8.0
Stage (Feet-NGVD)
2.0 0.0 -4.0 -6.0 -8.0 -10.0 -12.0 -14.0 -16.0 -18.0 -22.0 -24.0 -26.0
0 100 200 300 400
Width (Meters)

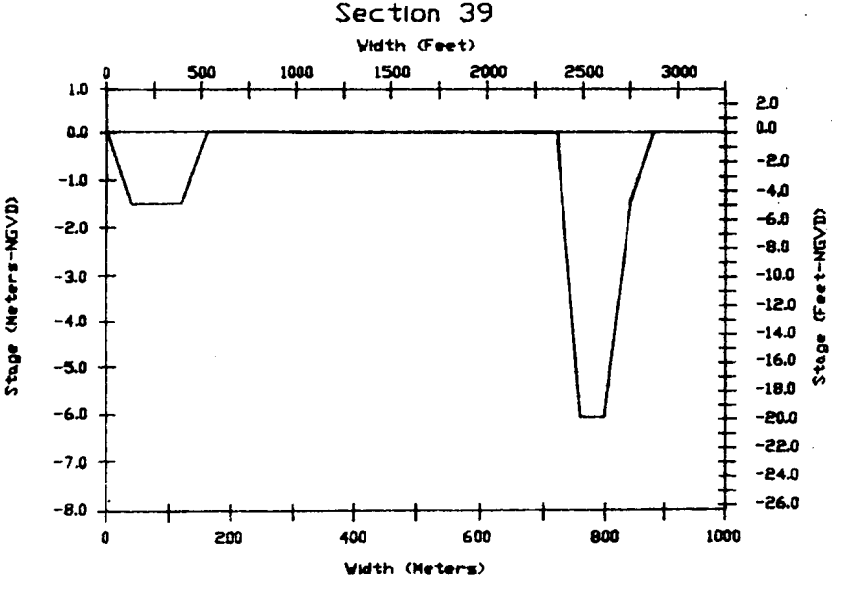
Section 39
Width (Feet)
0 500 1000 1500 2000 2500 3000
Stage (Meters-NGVD)
1.0 0.0 -1.0 -2.0 -3.0 -4.0 -5.0 -6.0 -7.0 -8.0
Stage (Feet-NGVD)
2.0 0.0 -2.0 -4.0 -6.0 -8.0 -10.0 -12.0 -14.0 -16.0 -18.0 -20.0 -22.0 -24.0 -26.0
0 200 400 600 800 1000
Width (Meters)

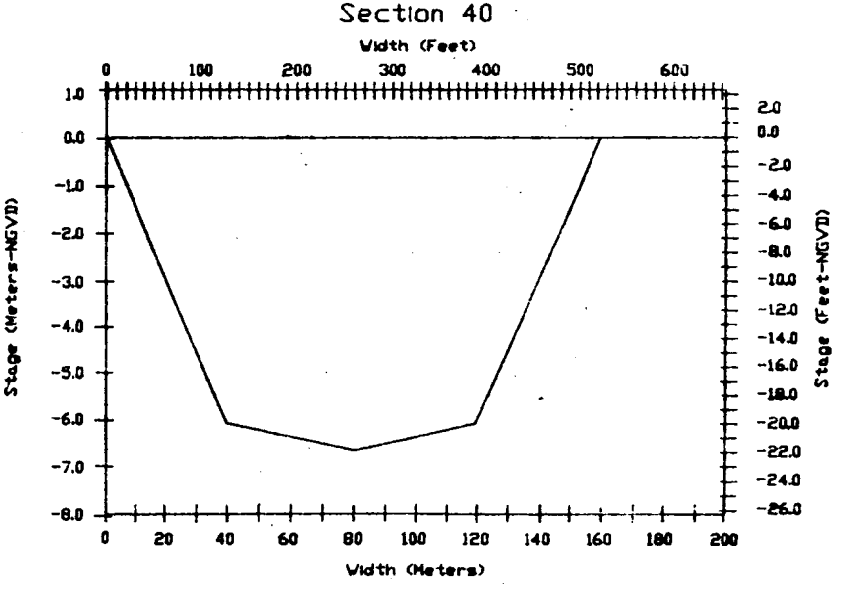
Section 40
Width (Feet)
0 100 200 300 400 500 600
Stage (Meters-NGVD)
1.0 0.0 -1.0 -2.0 -3.0 -4.0 -5.0 -6.0 -7.0 -8.0
Stage (Feet-NGVD)
2.0 0.0 -2.0 -4.0 -6.0 -8.0 -10.0 -12.0 -14.0 -16.0 -18.0 -20.0 -22.0 -24.0 -26.0
0 20 40 60 80 100 120 140 160 180 200
Width (Meters)